

Optimization of Beyond Diagonal RIS: A Universal Framework Applicable to Arbitrary Architectures

Zheyu Wu and Bruno Clerckx

Abstract—Reconfigurable intelligent surfaces (RISs) are envisioned as a promising technology for future wireless communication systems due to their ability to control the propagation environment in a hardware- and energy-efficient way. Recently, the concept of RISs has been extended to beyond diagonal RISs (BD-RISs), which unlock the full potential of RISs thanks to the presence of tunable interconnections between RIS elements. While various algorithms have been proposed for specific BD-RIS architectures, a universal optimization framework applicable to arbitrary architectures is still lacking. In this paper, we bridge this research gap by proposing an architecture-independent framework for BD-RIS optimization, with the main focus on sum-rate maximization and transmit power minimization in multiuser multi-input single-output (MU-MISO) systems. Specifically, we first incorporate BD-RIS architectures into the models by connecting the scattering matrix with the admittance matrix and introducing appropriate constraints to the admittance matrix. The formulated problems are then solved by our custom-designed partially proximal alternating direction method of multipliers (pp-ADMM) algorithms. The pp-ADMM algorithms are computationally efficient, with each subproblem either admitting a closed-form solution or being easily solvable. We further explore the extension of the proposed framework to general utility functions and multiuser multi-input multi-output (MU-MIMO) systems. Simulation results demonstrate that the proposed approaches achieve a better trade-off between performance and computational efficiency compared to existing methods. We also compare the performance of various BD-RIS architectures in MU-MISO systems using the proposed approach, which has not been explored before due to the lack of an architecture-independent framework.

Index Terms—Alternating direction method of multipliers, architecture independent, beyond diagonal reconfigurable intelligent surface, sum-rate maximization, transmit power minimization

I. INTRODUCTION

Reconfigurable intelligent surfaces (RISs) [1]–[4] are envisioned as a promising technology to enhance the performance and coverage of future wireless communication systems. A RIS consists of numerous near-passive reconfigurable elements that can be coordinated to dynamically shape the propagation environment. Compared to traditional active devices like antennas or relays, RISs operate with significantly lower cost and power, making them a sustainable solution that meets the growing demand for low-cost, energy-efficient, and high-performance wireless networks in 6G and beyond.

In a conventional RIS, each reconfigurable element is individually connected to its own load to ground without any

inter-element connection, which results in a diagonal scattering matrix — also referred to as a phase shift matrix in the literature. Very recently, Beyond Diagonal RISs (BD-RISs) have emerged as an advanced generalization of conventional RISs [5], [6]. By allowing interconnections between different reconfigurable elements through tunable impedances, BD-RISs are able to achieve scattering matrices not limited to being diagonal, offering greater flexibility in beam control. Different circuit topologies of inter-element connections result in different BD-RIS architectures. The fully-connected RIS, in which every pair of reconfigurable elements is inter-connected, offers the highest design flexibility but also entails the highest circuit complexity [5]. To mitigate the high complexity of fully-connected RISs, group-connected architectures have been introduced in [5], [7]. Furthermore, two novel BD-RIS architectures, known as tree-connected and forest-connected RISs, have been developed in [8] and [9] using graph theory and have been shown to achieve the performance-complexity Pareto frontier in single-user multi-input single-output (MISO) systems.

A rich body of research has demonstrated the advantages of BD-RISs over conventional RISs in multiple aspects. BD-RIS is needed to achieve the upper bound on power/SNR maximization [5] and is hence also needed to achieve any information theoretic bound of RIS-aided multiuser or multi-antenna systems. Beyond this, BD-RIS offers numerous additional benefits, including boosting received signal power and sum-rate [5], [6], supporting various operational modes (reflective/transmissive/hybrid) [7], expanding coverage [10], reducing the number of resolution bits [11], achieving better capability to overcome mutual coupling [12], [13], etc. The potential of BD-RISs has also been explored in TDD duplex systems (for channel attack) [14], wideband communication systems [15]–[17], full-duplex systems [18], dual-function radar-communication (DFRC) systems [19], unmanned aerial vehicle (UAV) systems [20], and rate-splitting multiple access (RSMA) systems [21], [22]. Furthermore, several extensions of BD-RIS have been proposed to enhance its performance, such as new grouping strategies adaptive to channel state information (CSI) [23], [24], a distributed BD-RIS deployment that is less susceptible to lossy interconnections [25], and a BD-RIS aided stacked intelligent metasurface with improved wave manipulation capabilities [26].

Despite the great benefits offered by BD-RISs, their optimization is far more challenging than that of conventional RISs. First, the more complicated circuit topology of BD-RISs introduces more complicated objective functions and constraints to the corresponding optimization problems, such

Z. Wu and B. Clerckx are with the Department of Electrical and Electronic Engineering, Imperial College London, London, SW7 2AZ, U.K. (email: {zheyu.wu, b.clerckx}@imperial.ac.uk). This work has been partially supported by UKRI grant EP/Y004086/1, EP/X040569/1, EP/Y037197/1, EP/X04047X/1, EP/Y037243/1.

as unitary and/or symmetric constraints [5], [7], [10], [16]–[24], [27] and constraints/objective functions involving matrix inversion [8], [9], [11]–[13], [15], [25]. Second, the number of variables increases dramatically due to the significantly larger number of impedances in BD-RISs. In fully-connected BD-RISs, for example, the number of impedances grows quadratically with the number of RIS elements. This imposes higher demands on algorithm efficiency.

Existing optimization strategies for BD-RIS can mainly be categorized into three types. The first type of approaches seeks the closed-form solution of the corresponding optimization problem [8], [9], [13], [28]. However, this method is applicable only in very limited scenarios, such as single-user single-input single-output (SISO) systems. The second type is heuristic approaches [29]. Specifically, the authors in [29] proposed a heuristic two-stage approach, which first determines the scattering matrix heuristically and then treat it as fixed in beamforming design. This kind of heuristic method, however, lacks theoretical support and does not offer any performance guarantees. The third type is optimization-based approaches, which leverages classical optimization techniques to tackle the complexities imposed by BD-RISs. Examples include employing manifold optimization for unitary constraints [7], [23], [30], applying penalty dual decomposition to handle unitary and symmetric constraints [31], applying Neumann series approximation [12] and quasi-Newton method [21] to deal with matrix inversion, etc. These approaches generally achieve satisfactory performance with theoretical guarantee, but at the expense of higher computational cost than heuristic approaches. The key to designing optimization-based approaches is to strike a balance between efficiency and effectiveness.

Although various approaches have been proposed for BD-RIS optimization in different scenarios, existing works have the following limitations. First and most importantly, they only work for specific BD-RIS architectures (mostly for group- and fully-connected BD-RISs [7], [29], [31]). To date, there still lacks a universal, i.e., architecture-independent, optimization framework applicable to all BD-RIS architectures in general multiuser systems. Second, existing algorithms are either heuristic [29] or time-consuming [31]. In particular, very few works deal with the transmit power minimization problem, possibly due to the technical challenges arising from the coupling of BD-RIS constraints with users' quality-of-service (QoS) constraints [31]. To the best of our knowledge, the only existing algorithm is [31], which, however, is computationally inefficient when the number of RIS elements is large.

Motivated by the aforementioned limitations, this paper aims to develop an efficient architecture-independent framework for BD-RIS optimization, considering both sum-rate maximization and transmit power minimization problems. The contributions are summarized as follows.

First, we formulate the sum-rate maximization and transmit power minimization problems for BD-RIS-aided multiuser MISO (MU-MISO) systems in an architecture-independent way such that the models can encompass any BD-RIS architecture. Specifically, building on microwave network theory and existing BD-RIS modeling [8], [32], we relate the scattering matrix with the admittance matrix and incorporate BD-RIS

architecture into the model by imposing proper constraints on the admittance matrix. This is in sharp contrast to all existing models for multiuser systems, which are specific to group- and fully-connected BD-RISs.

Second, we propose efficient partially proximal alternating direction method of multipliers (pp-ADMM) algorithms for solving the formulated problems. The idea is to first introduce appropriate auxiliary variables to make the problems amenable to the ADMM framework. This includes transforming the constraint involving matrix inversion into a low-dimensional bi-linear constraint, simplifying the sum-rate maximization problem with fractional programming (FP) technique, and decomposing the complicated QoS constraint in the transmit power minimization problem into a bilinear constraint and an easy-to-projection constraint. Then, the ADMM framework is applied to solve the transformed problems, with proximal terms incorporated for specific variables to ensure stability and convergence of the algorithms.

Third, we discuss the generalization of the proposed approach. Specifically, we extract an optimization framework to handle general utility functions and, in particular, explore its applicability to max-min fairness and energy efficiency maximization. Furthermore, we discuss the extension of the proposed framework to multiuser multi-input multi-output (MU-MIMO) systems.

To the best of our knowledge, the proposed approach is the first architecture-independent framework for BD-RIS optimization. In addition, simulation results demonstrate that, when applied to group- and fully-connected BD-RISs, our approach achieves a superior trade-off between sum-rate performance and computational efficiency compared to the existing state-of-the-art algorithms in [29], [31]. For the transmit power minimization problem, our approach attains lower transmit power with significantly reduced computational complexity than the only existing algorithm in [31].

Organization: The rest of the paper is organized as follows. We first introduce the system model and problem formulations in Section II. In Sections III and IV, we propose efficient pp-ADMM algorithms for solving the sum-rate maximization and transmit power minimization problems of BD-RIS-aided MU-MISO systems, respectively. In Section V, we discuss the generalization of the proposed optimization framework. The effectiveness and efficiency of the proposed approaches are verified through extensive simulations in Section VI. Finally, the paper is concluded in Section VII.

Notations: Throughout the paper, \mathbb{C} and \mathbb{R} denote the complex space and the real space, respectively. We use x , \mathbf{x} , \mathbf{X} , and \mathcal{X} to represent a scalar, column vector, matrix, and set, respectively. For a matrix \mathbf{X} , $\mathbf{X}_{\mathcal{S}_1, \mathcal{S}_2}$ denotes its submatrix with rows indexed by \mathcal{S}_1 and columns indexed by \mathcal{S}_2 , where $\mathbf{X}(\mathcal{S}_1, \mathcal{S}_2)$ is also used in certain context to avoid possible confusion. In particular, $X_{n,m}$ denotes the (n, m) -th entry of \mathbf{X} . The operators $(\cdot)^T$, $(\cdot)^\dagger$, $(\cdot)^{-1}$, $\mathcal{R}(\cdot)$, and $\mathcal{I}(\cdot)$ return the transpose, the Hermitian transpose, the inverse, the real part, and the imaginary part of their corresponding argument, respectively. Given two vectors $\mathbf{x} \in \mathbb{C}^n$ and $\mathbf{y} \in \mathbb{C}^n$, $\langle \mathbf{x}, \mathbf{y} \rangle$ represents their inner product, i.e., $\langle \mathbf{x}, \mathbf{y} \rangle = \mathcal{R}(\mathbf{x}^\dagger \mathbf{y})$. For two sets \mathcal{X}_1 and \mathcal{X}_2 , $\mathcal{X}_1 \setminus \mathcal{X}_2$ denotes the difference between \mathcal{X}_1 and

\mathcal{X}_2 . The notation $\|\cdot\|_2$ refers to the ℓ_2 -norm of a vector or the spectral norm of a matrix, and $\|\cdot\|_F$ denotes the Frobenius norm of a matrix. The operator $|\cdot|$ returns the modulus if applied to a scalar and the number of elements if applied to a set. The symbol \mathbf{I}_n refers to an n -dimensional identity matrix. Finally, i represents the imaginary unit.

II. PROBLEM FORMULATION

A. System Model

Consider a BD-RIS-aided MU-MISO system¹, where a base station (BS) with N transmit antennas serves K single-antenna users simultaneously with the assistance of an M -element BD-RIS. As in [5], the M -element BD-RIS can be modeled as M antennas connected to an M -port reconfigurable impedance network, which induces a non-diagonal scattering matrix $\Theta \in \mathbb{C}^{M \times M}$ to control the propagation of the incident waveform. Denote $\mathbf{s} = [s_1, s_2, \dots, s_K]^T$ as the data symbol vector for the users with $\mathbb{E}[\mathbf{s}\mathbf{s}^\dagger] = \mathbf{I}_K$, and let $\mathbf{W} = [\mathbf{w}_1, \mathbf{w}_2, \dots, \mathbf{w}_K] \in \mathbb{C}^{N \times K}$ be the beamforming matrix. Then the received signal at the k -th user can be expressed as²

$$r_k = \mathbf{h}_k^\dagger \Theta \mathbf{G} \sum_{k=1}^K \mathbf{w}_k s_k + n_k, \quad k = 1, 2, \dots, K, \quad (1)$$

where $\mathbf{G} \in \mathbb{C}^{M \times N}$ is the channel matrix between the BS and the BD-RIS, $\mathbf{h}_k \in \mathbb{C}^M$ denotes the channel vector between the BD-RIS and the k -th user, and $n_k \sim \mathcal{CN}(0, \sigma^2)$ is the additive white Gaussian noise. For simplicity, we neglect the direct channel between the BS and the users; however, all results can be straightforwardly generalized to scenarios where the direct channel is taken into account.

Our goal in this paper is to develop a framework for jointly optimizing the beamforming matrix \mathbf{W} and the scattering matrix Θ , in a universal manner such that the framework is architecture-independent, i.e., it is applicable to any given BD-RIS architecture. For this purpose, we resort to the microwave network theory [33] and relates the scattering matrix Θ (i.e., the S -parameter) with the admittance matrix $\mathbf{Y} \in \mathbb{C}^{M \times M}$ (i.e., the Y -parameter) as

$$\Theta = (\mathbf{I} + Z_0 \mathbf{Y})^{-1} (\mathbf{I} - Z_0 \mathbf{Y}),$$

where Z_0 denotes the reference impedance, usually set as $Z_0 = 50 \Omega$. To maximize the reflected power of BD-RIS, \mathbf{Y} should be a purely imaginary matrix, denoted as $\mathbf{Y} = i\mathbf{B}$, where $\mathbf{B} \in \mathbb{R}^{M \times M}$ denotes the susceptance matrix of the reconfigurable impedance network. Equivalently, this amounts to a unitary constraint on Θ , i.e., $\Theta^\dagger \Theta = \mathbf{I}_M$. As commonly assumed in the literature, the reconfigurable impedance network is considered reciprocal, leading to symmetric constraints on the admittance and scattering matrices³, i.e., $\mathbf{B} = \mathbf{B}^T$, $\mathbf{Y} = \mathbf{Y}^T$, and $\Theta = \Theta^T$.

¹We discuss the generalization of the proposed approach to the MU-MIMO system in Section V.

²In this paper, we assume perfect matching, no mutual coupling, no structural scattering or specular reflection, and that the unilateral approximation holds [32].

³For non-reciprocal RISs, there is no symmetric constraint, which simplifies the corresponding optimization problem. Our proposed framework is directly applicable in this case.

The Y -parameter has the advantage of being able to characterize the circuit topology of BD-RISs. Specifically, denote the admittance for the n -th port of the reconfigurable impedance network as \bar{Y}_n , and denote the admittance connecting the n -th and m -th ports as $\bar{Y}_{n,m}$. Then according to [8], the admittance matrix \mathbf{Y} of the reconfigurable impedance network is given by

$$Y_{n,m} = \begin{cases} -\bar{Y}_{n,m}, & \text{if } n \neq m; \\ \bar{Y}_n + \sum_{j \neq n} \bar{Y}_{n,j}, & \text{if } n = m. \end{cases}$$

Clearly, for $n \neq m$, $Y_{n,m}$ is nonzero if and only if $\bar{Y}_{n,m}$ is nonzero. Therefore, the interconnections between different ports in the reconfigurable impedance network are represented by the non-zero elements in \mathbf{Y} , allowing it to characterize any arbitrary BD-RIS architecture⁴.

In the following, we review several popular BD-RIS architectures proposed in the existing literature (see also Fig. 1).

B. Different RIS Architectures

1) *Single-Connected RIS*: When there is no interconnection between different ports, i.e., $Y_{n,m} = 0$ for all $n \neq m$, the BD-RIS reduces to the traditional diagonal RIS, also known as a single-connected RIS, which has been extensively studied in literature. In this case, \mathbf{Y} and Θ are both diagonal, i.e.,

$$\begin{aligned} \mathbf{Y} &= \text{diag}(Y_1, Y_2, \dots, Y_M), \\ \Theta &= \text{diag}(\Theta_1, \Theta_2, \dots, \Theta_M). \end{aligned}$$

2) *Fully-Connected RIS*: When there is an impedance connecting each pair of ports, the corresponding architecture is referred to as a fully-connected RIS. In this case, both \mathbf{Y} and Θ are full matrices, i.e., $Y_{n,m} \neq 0$ and $\Theta_{n,m} \neq 0$ for all $n, m \in \{1, 2, \dots, M\}$. The fully-connected RIS offers the highest design flexibility but also suffers from the highest circuit complexity.

3) *Group-Connected RIS*: The group-connected RIS has been proposed to achieve a favorable trade-off between system performance and circuit complexity [7]. In group-connected RIS, the RIS elements are divided into multiple groups, where each group employs a fully-connected architecture, and no connections exist between different groups. Let G denote the number of groups; then each group has a number of $N_G = M/G$ RIS elements, which we refer to as the group size. In this case, both \mathbf{Y} and Θ exhibit a block diagonal structure:

$$\begin{aligned} \mathbf{Y} &= \text{blkdiag}(\mathbf{Y}_1, \mathbf{Y}_2, \dots, \mathbf{Y}_G), \\ \Theta &= \text{blkdiag}(\Theta_1, \Theta_2, \dots, \Theta_G). \end{aligned}$$

In particular, a group-connected RIS becomes a fully-connected RIS when $G = 1$ and reduces to a single-connected RIS when $G = M$.

4) *Tree-Connected RIS*: In [8], the circuit topology of BD-RIS is characterized by a graph $\mathcal{G} = (\mathcal{V}, \mathcal{E})$, where the vertices $\mathcal{V} := \{V_1, V_2, \dots, V_M\}$ represents the ports of the reconfigurable impedance network, and the edges $\mathcal{E} := \{(V_i, V_j) \mid Y_{i,j} \neq 0, i \neq j\}$ record all the interconnections

⁴This property does not hold for the S - or Z -parameter, as the mapping from the admittance matrix \mathbf{Y} to the scattering matrix Θ or the impedance matrix \mathbf{Z} is inherently non-linear.

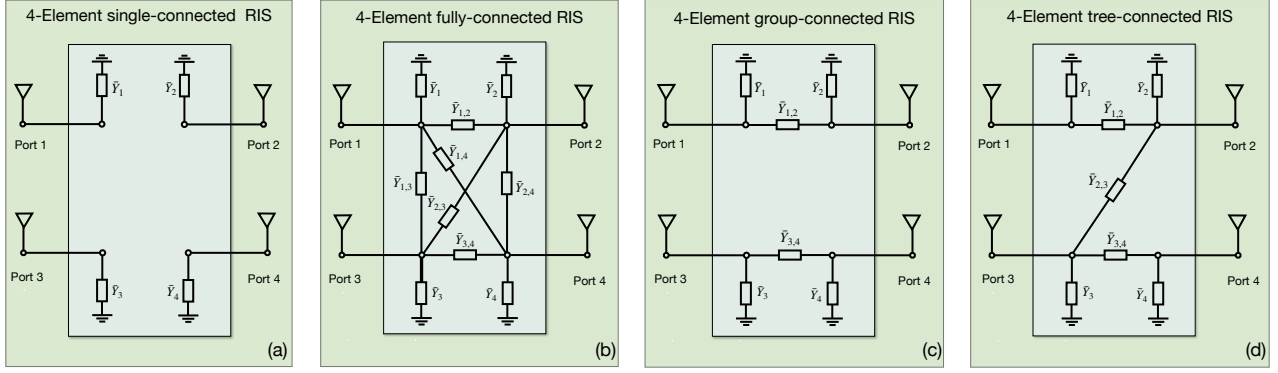


Fig. 1. Different BD-RIS architectures, where (a) single-connected RIS, (b) fully-connected RIS, (c) group-connected RIS, (d) tree-connected RIS.

between different ports. Tree-connected RISs refer to a class of BD-RIS architectures whose corresponding graph is a tree [8]. One example of tree-connected RISs is the tridiagonal RIS [8], whose circuit topology forms a path graph, and the corresponding admittance matrix is a tridiagonal matrix given by

$$\mathbf{Y} = \begin{bmatrix} Y_{1,1} & Y_{1,2} & & & \\ Y_{1,2} & Y_{2,2} & \ddots & & \\ & \ddots & \ddots & \ddots & \\ & & & Y_{M-1,M} & \\ & & & Y_{M-1,M} & Y_{M,M} \end{bmatrix}. \quad (2)$$

Note that for a tree-connected RIS, there is no clear structure for its scattering matrix Θ . This demonstrates the advantage of using Y -parameter, as discussed earlier.

It has been proved in [8] that the tree-connected RIS is optimal for single-user MISO systems, which achieves the same performance as fully-connected ones while maintaining the lowest circuit complexity. However, its performance in more practical multiuser systems remains unknown.

C. Problem Formulation

With the system model in (1), the signal-to-interference-plus-noise ratio (SINR) of the k -th user is

$$\text{SINR}_k(\Theta, \mathbf{W}) = \frac{|\mathbf{h}_k^\dagger \Theta \mathbf{G} \mathbf{w}_k|^2}{\sum_{j \neq k} |\mathbf{h}_k^\dagger \Theta \mathbf{G} \mathbf{w}_j|^2 + \sigma^2}, \quad k = 1, 2, \dots, K. \quad (3)$$

To account for different BD-RIS architectures, we introduce the following notation:

$$\mathcal{B} = \{\mathbf{B} \in \mathbb{R}^{M \times M} \mid B_{i,j} = 0, \text{ if there is no interconnection between the } i\text{-th and } j\text{-th ports, } i \neq j\},$$

i.e., the set \mathcal{B} collects all susceptance matrices corresponding to a specific architecture.

In this paper, we mainly focus on two different problem formulations: sum-rate maximization under the total transmit power constraint and transmit power minimization under users' QoS constraints. The proposed framework, however, can be generalized to accommodate other utility functions; see discussions in Section V.

1) *Sum-rate Maximization*: Based on the above discussions, the sum-rate maximization problem can be formulated as

$$\max_{\mathbf{W}, \Theta, \mathbf{B}} \sum_{k=1}^K \log(1 + \text{SINR}_k(\Theta, \mathbf{W})) \quad (4a)$$

$$\text{s.t. } \Theta = (\mathbf{I} + iZ_0 \mathbf{B})^{-1} (\mathbf{I} - iZ_0 \mathbf{B}), \quad (4b)$$

$$\mathbf{B} = \mathbf{B}^T, \quad \mathbf{B} \in \mathcal{B}, \quad (4c)$$

$$\|\mathbf{W}\|_F^2 \leq P_T, \quad (4d)$$

where constraint (4b) relates the scattering matrix Θ with \mathbf{B} , constraint (4c) is to ensure that the reconfigurable impedance network is reciprocal and complies with the specified architecture, and (4d) is the transmit power constraint with P_T being the maximum transmit power.

2) *Transmit Power Minimization*: The transmit power minimization problem is formulated as

$$\min_{\mathbf{W}, \Theta, \mathbf{B}} \|\mathbf{W}\|_F^2 \quad (5a)$$

$$\text{s.t. } \text{SINR}_k(\Theta, \mathbf{W}) \geq \Gamma_k, \quad k = 1, 2, \dots, K, \quad (5b)$$

$$\Theta = (\mathbf{I} + iZ_0 \mathbf{B})^{-1} (\mathbf{I} - iZ_0 \mathbf{B}), \quad (5c)$$

$$\mathbf{B} = \mathbf{B}^T, \quad \mathbf{B} \in \mathcal{B}, \quad (5d)$$

where $\Gamma_k > 0$ is the pre-specified SINR threshold for user k .

Both the sum-rate maximization and transmit power minimization problems have been extensively studied in traditional MU-MISO systems [34]–[37] and diagonal RIS-aided MU-MISO systems [1]–[4]. However, in the context of BD-RIS, the constraints are significantly more complicated, introducing new challenges for algorithm design. Specifically, the expression of the scattering matrix in (4b) and (5c) involves matrix inversion, which is further coupled with the beamforming matrix in the non-convex SINR expression (and the logarithmic function). The large dimensions of Θ and \mathbf{B} , arising from the numerous impedances in BD-RIS, exacerbate the challenges. In the following two sections, we will propose two efficient algorithms for solving problems (4) and (5) by carefully exploiting the structure of the problems.

III. SUM-RATE MAXIMIZATION PROBLEM

In this section, we propose an efficient algorithm for solving the sum-rate maximization problem in (4). First, we transform (4) into a more amenable form in Section III-A, which is then solved by a custom-designed partially proximal ADMM

(pp-ADMM) algorithm in Section III-B. The complexity and convergence analysis of the proposed pp-ADMM algorithm is given in Section IV-C.

A. Equivalent Reformulation

An important observation we can draw from the SINR expression in (3) is that the scattering matrix Θ appears in conjunction with the channel vectors $\{\mathbf{h}_k\}_{k=1}^K$. Motivated by this, we introduce auxiliary variables $\mathbf{u}_k = \Theta^\dagger \mathbf{h}_k \in \mathbb{C}^M$ for $k = 1, 2, \dots, K$, with which the SINR of user k can be expressed as a function of \mathbf{u}_k and \mathbf{W} as

$$\text{SINR}(\mathbf{u}_k, \mathbf{W}) = \frac{|\mathbf{u}_k^\dagger \mathbf{G} \mathbf{w}_k|^2}{\sum_{j \neq k} |\mathbf{u}_k^\dagger \mathbf{G} \mathbf{w}_j|^2 + \sigma^2}, \quad (6)$$

and problem (4) is transformed into the following equivalent form:

$$\max_{\mathbf{W}, \mathbf{B}, \mathbf{U}} R(\mathbf{W}, \mathbf{U}) := \sum_{k=1}^K \log(1 + \text{SINR}_k(\mathbf{u}_k, \mathbf{W})) \quad (7a)$$

$$\text{s.t.} \quad (\mathbf{I} - iZ_0 \mathbf{B}) \mathbf{U} = (\mathbf{I} + iZ_0 \mathbf{B}) \mathbf{H}, \quad (7b)$$

$$\mathbf{B} = \mathbf{B}^T, \quad \mathbf{B} \in \mathcal{B}, \quad (7c)$$

$$\|\mathbf{W}\|_F^2 \leq P_T, \quad (7d)$$

where $\mathbf{H} = [\mathbf{h}_1, \mathbf{h}_2, \dots, \mathbf{h}_K]$ and $\mathbf{U} = [\mathbf{u}_1, \mathbf{u}_2, \dots, \mathbf{u}_K]$. The advantage of this new formulation is twofold. First, there is no longer any matrix inversion in the constraints. The complicated constraint involving matrix inversion in (4b) is transformed into the bi-linear constraint in (7b), which is more trackable. Second, it greatly reduces the dimension of both the optimization variables and constraints: the variable $\Theta \in \mathbb{C}^{M \times M}$ is eliminated and replaced by the auxiliary variable $\mathbf{U} \in \mathbb{C}^{M \times K}$, and the M^2 -dimensional constraint in (4b) is replaced by the MK -dimensional constraint in (7b), where we note that in practice, $M \gg K$.

Since the objective function (7a) is still complicated, we employ the FP technique [38], [39] to rewrite it into the following equivalent form:

$$R(\mathbf{W}, \mathbf{U}) = \max_{\mathbf{y}, \gamma} \tilde{R}(\mathbf{y}, \gamma, \mathbf{W}, \mathbf{U}), \quad (8)$$

where

$$\begin{aligned} \tilde{R}(\mathbf{y}, \gamma, \mathbf{W}, \mathbf{U}) &= \sum_{k=1}^K \log(1 + \gamma_k) - \gamma_k \\ &+ (1 + \gamma_k) \left(2 \langle \mathbf{y}_k, \mathbf{u}_k^\dagger \mathbf{G} \mathbf{w}_k \rangle - |\mathbf{y}_k|^2 \left(\sum_{j=1}^K |\mathbf{u}_k^\dagger \mathbf{G} \mathbf{w}_j|^2 + \sigma^2 \right) \right). \end{aligned}$$

With the above transformation, problem (7) can be equivalently expressed as

$$\begin{aligned} \max_{\mathbf{y}, \gamma, \mathbf{W}, \mathbf{B}, \mathbf{U}} \quad & \tilde{R}(\mathbf{y}, \gamma, \mathbf{W}, \mathbf{U}) \\ \text{s.t.} \quad & (7b) - (7d). \end{aligned} \quad (9)$$

Problems (7) and (9) are equivalent in the sense that given any optimal solution $(\mathbf{W}^*, \mathbf{B}^*, \mathbf{U}^*)$ of problem (7), $(\mathbf{y}^*, \gamma^*, \mathbf{W}^*, \mathbf{B}^*, \mathbf{U}^*)$ with

$$\mathbf{y}_k^* = \frac{\mathbf{u}_k^{*\dagger} \mathbf{G} \mathbf{w}_k^*}{\sum_{j=1}^K |\mathbf{u}_k^{*\dagger} \mathbf{G} \mathbf{w}_j^*|^2 + \sigma^2} \quad \text{and} \quad \gamma_k^* = \frac{|\mathbf{u}_k^{*\dagger} \mathbf{G} \mathbf{w}_k^*|^2}{\sum_{j \neq k} |\mathbf{u}_k^{*\dagger} \mathbf{G} \mathbf{w}_j^*|^2 + \sigma^2}$$

is an optimal solution of problem (9), and vice versa [39].

B. pp-ADMM Algorithm for Solving (9)

Compared to the original problem (4), problem (9) is much easier to tackle. Its objective function $\tilde{R}(\mathbf{y}, \gamma, \mathbf{W}, \mathbf{U})$ is concave and straightforward to optimize with respect to each variable block when the other blocks are fixed. The only remaining challenge lies in the bilinear constraint (7b) that couples variables \mathbf{B} and \mathbf{U} . To deal with this, we resort to the ADMM framework, which is well-suited for addressing problems with such a structure [40], [41].

In the following, we propose a partially proximal ADMM (pp-ADMM) algorithm for solving (9). First, the Lagrangian function of (9) is given by

$$\begin{aligned} \mathcal{L}_\rho(\mathbf{y}, \gamma, \mathbf{W}, \mathbf{B}, \mathbf{U}, \boldsymbol{\lambda}) \\ = \tilde{R}(\mathbf{y}, \gamma, \mathbf{W}, \mathbf{U}) - \langle \boldsymbol{\lambda}, (\mathbf{I} - iZ_0 \mathbf{B}) \mathbf{U} - (\mathbf{I} + iZ_0 \mathbf{B}) \mathbf{H} \rangle \\ - \frac{\rho}{2} \|(\mathbf{I} - iZ_0 \mathbf{B}) \mathbf{U} - (\mathbf{I} + iZ_0 \mathbf{B}) \mathbf{H}\|_F^2, \end{aligned} \quad (10)$$

where $\boldsymbol{\lambda} \in \mathbb{C}^{M \times K}$ is the Lagrange multiplier and ρ is the penalty parameter. The proposed pp-ADMM algorithm is given as follows.

$$\mathbf{y}^{t+1} \in \arg \max \mathcal{L}_\rho(\mathbf{y}, \gamma^t, \mathbf{W}^t, \mathbf{B}^t, \mathbf{U}^t, \boldsymbol{\lambda}^t), \quad (11a)$$

$$\gamma^{t+1} \in \arg \max \mathcal{L}_\rho(\mathbf{y}^{t+1}, \gamma, \mathbf{W}^t, \mathbf{B}^t, \mathbf{U}^t, \boldsymbol{\lambda}^t), \quad (11b)$$

$$\mathbf{W}^{t+1} \in \arg \max_{\|\mathbf{W}\|_F^2 \leq P_T} \mathcal{L}_\rho(\mathbf{y}^{t+1}, \gamma^{t+1}, \mathbf{W}, \mathbf{B}^t, \mathbf{U}^t, \boldsymbol{\lambda}^t) - \frac{\tau}{2} \|\mathbf{W} - \mathbf{W}^t\|_F^2, \quad (11c)$$

$$\mathbf{B}^{t+1} \in \arg \max_{\substack{\mathbf{B} = \mathbf{B}^T \\ \mathbf{B} \in \mathcal{B}}} \mathcal{L}_\rho(\mathbf{y}^{t+1}, \gamma^{t+1}, \mathbf{W}^{t+1}, \mathbf{B}, \mathbf{U}^t, \boldsymbol{\lambda}^t) - \frac{\xi}{2} \|\mathbf{B} - \mathbf{B}^t\|_F^2, \quad (11d)$$

$$\mathbf{U}^{t+1} \in \arg \max \mathcal{L}_\rho(\mathbf{y}^{t+1}, \gamma^{t+1}, \mathbf{W}^{t+1}, \mathbf{B}^{t+1}, \mathbf{U}, \boldsymbol{\lambda}^t), \quad (11e)$$

$$\boldsymbol{\lambda}^{t+1} = \boldsymbol{\lambda}^t + \rho((\mathbf{I} - iZ_0 \mathbf{B}^{t+1}) \mathbf{U}^{t+1} - (\mathbf{I} + iZ_0 \mathbf{B}^{t+1}) \mathbf{H}). \quad (11f)$$

Different from classical ADMM, we incorporate proximal terms in the updates of \mathbf{W} and \mathbf{B} , where τ and ξ are the corresponding proximal parameters. The aim is to enhance stability and ensure convergence of the proposed algorithm. Further details are provided in Section III-B3 and Section III-B4. We next detail the update of each variable.

1) *Update of \mathbf{y}* : The \mathbf{y} -subproblem (11a) is unconstrained and quadratic, admitting a closed-form solution as

$$\mathbf{y}_k^{t+1} = \frac{(\mathbf{u}_k^t)^\dagger \mathbf{G} \mathbf{w}_k^t}{\sum_{j=1}^K |(\mathbf{u}_k^t)^\dagger \mathbf{G} \mathbf{w}_j^t|^2 + \sigma^2}, \quad k = 1, 2, \dots, K. \quad (12)$$

2) *Update of γ* : The γ -subproblem (11b) is strictly concave. By setting the derivative of $\tilde{R}(\mathbf{y}^{t+1}, \gamma, \mathbf{W}^t, \mathbf{U}^t)$ with respect to γ to zero and solving the corresponding equation, it is easy to obtain the following closed-form solution:

$$\gamma_k^{t+1} = \frac{|(\mathbf{u}_k^t)^\dagger \mathbf{G} \mathbf{w}_k^t|^2}{\sum_{j \neq k} |(\mathbf{u}_k^t)^\dagger \mathbf{G} \mathbf{w}_j^t|^2 + \sigma^2}, \quad k = 1, 2, \dots, K. \quad (13)$$

3) *Update of \mathbf{W}* : The \mathbf{W} -subproblem can be written as

$$\min_{\|\mathbf{W}\|_F^2 \leq P_T} \sum_{k=1}^K \left(\mathbf{w}_k^\dagger \mathbf{Q} \mathbf{w}_k - 2 \langle \mathbf{c}_k, \mathbf{w}_k \rangle \right) + \frac{\tau}{2} \|\mathbf{W} - \mathbf{W}^t\|_F^2, \quad (14)$$

where $\mathbf{Q} = \sum_{j=1}^K (1 + \gamma_j^{t+1}) |y_j^{t+1}|^2 \mathbf{G}^\dagger \mathbf{u}_j^t (\mathbf{u}_j^t)^\dagger \mathbf{G}$ and $\mathbf{c}_k = y_k^{t+1} (1 + \gamma_k^{t+1}) \mathbf{G}^\dagger \mathbf{u}_k^t$ (in the notations \mathbf{Q} and \mathbf{c}_k , we omit their

dependance on t for simplicity). Note that $\mathbf{Q} \in \mathbb{C}^{N \times N}$ is a summation of K rank-one matrices, and thus has a rank of at most K . This implies that when $N > K$, i.e., the number of transmit antennas is larger than the number of users in the system, \mathbf{Q} is rank deficient. The proximal term is introduced to ensure that the objective function of (14) is strongly convex, which is important to the convergence of the algorithm.

Problem (14) is a quadratically constrained quadratic programming (QCQP), which can be efficiently solved via a one-dimensional bisection search. Based on the first-order optimality condition of (14), its solution can be expressed as

$$\mathbf{w}_k^{t+1} = \left(\mathbf{Q} + \left(\frac{\tau}{2} + \eta^* \right) \mathbf{I}_N \right)^{-1} \left(\mathbf{c}_k + \frac{\tau}{2} \mathbf{w}_k^t \right), \quad k = 1, 2, \dots, K,$$

where $\eta^* \geq 0$ is the Lagrange multiplier associated with the total transmit power constraint and is determined according to the complementary slackness condition. Specifically, let

$$\mathbf{w}_k(\eta) = \left(\mathbf{Q} + \left(\frac{\tau}{2} + \eta \right) \mathbf{I}_N \right)^{-1} \left(\mathbf{c}_k + \frac{\tau}{2} \mathbf{w}_k^t \right).$$

Then $\eta^* = 0$ if $\sum_{k=1}^K \|\mathbf{w}_k(0)\|^2 \leq P_T$ and η^* is the solution to

$$\sum_{k=1}^K \|\mathbf{w}_k(\eta)\|^2 = P_T \quad (15)$$

otherwise. Equation (15) can be efficiently solved via a one-dimensional bisection search by rewriting it as

$$\sum_{n=1}^N \frac{\|\phi_n\|^2}{(d_n + \tau/2 + \eta)^2} = P_T,$$

where ϕ_n^T is the n -th row of the matrix $\mathbf{U}^\dagger [\mathbf{c}_1 + \tau \mathbf{w}_1^t/2, \mathbf{c}_2 + \tau \mathbf{w}_2^t/2, \dots, \mathbf{c}_K + \tau \mathbf{w}_K^t/2]$, and $\mathbf{Q} = \mathbf{U} \mathbf{D} \mathbf{U}^\dagger$ is the eigenvalue decomposition of \mathbf{Q} with $\mathbf{D} = \text{diag}(d_1, d_2, \dots, d_N)$; see more details in [35].

4) *Update of \mathbf{B}* : The \mathbf{B} -subproblem (11d) has the following form:

$$\min_{\substack{\mathbf{B}=\mathbf{B}^T \\ \mathbf{B} \in \mathcal{B}}} \left\| \mathbf{B}(iZ_0 \mathbf{U}^t + iZ_0 \mathbf{H}) - \left(\mathbf{U}^t - \mathbf{H} + \frac{\boldsymbol{\lambda}^t}{\rho} \right) \right\|_F^2 + \frac{\xi}{2} \|\mathbf{B} - \mathbf{B}^t\|_F^2. \quad (16)$$

Since variable \mathbf{B} is real-valued, it is convenient to transform (16) into the real space as

$$\min_{\mathbf{B}=\mathbf{B}^T, \mathbf{B} \in \mathcal{B}} \|\mathbf{B} \mathbf{M} - \boldsymbol{\Gamma}\|_F^2 + \frac{\xi}{2} \|\mathbf{B} - \mathbf{B}^t\|_F^2, \quad (17)$$

where

$$\mathbf{M} = [\mathcal{R}(iZ_0 \mathbf{U}^t + iZ_0 \mathbf{H}), \mathcal{I}(iZ_0 \mathbf{U}^t + iZ_0 \mathbf{H})] \in \mathbb{R}^{M \times 2K}$$

and

$$\boldsymbol{\Gamma} = [\mathcal{R}(\mathbf{U}^t - \mathbf{H} + \boldsymbol{\lambda}^t/\rho), \mathcal{I}(\mathbf{U}^t - \mathbf{H} + \boldsymbol{\lambda}^t/\rho)] \in \mathbb{R}^{M \times 2K}.$$

Due to the symmetry of \mathbf{B} and the constraint $\mathbf{B} \in \mathcal{B}$, the unknowns in \mathbf{B} are actually all its non-zero upper tridiagonal elements. Let

$$\mathbf{x} = [\mathbf{B}_{1, \mathcal{S}_1}, \mathbf{B}_{2, \mathcal{S}_2}, \dots, \mathbf{B}_{M, \mathcal{S}_M}]^T \quad (18)$$

with

$$\mathcal{S}_i = \{i, i+1, \dots, M\} \setminus \{j \mid j > i, B_{i,j} = 0\},$$

i.e., \mathbf{x} collects all the non-zero elements in the upper tridiagonal of \mathbf{B} . Then problem (17) can be equivalently expressed as an unconstrained quadratic programming over \mathbf{x} . Specifically, let $\{\mathbf{a}_m^T\}_{m=1}^M$ denote the rows of \mathbf{M} , i.e., $\mathbf{M}^T = [\mathbf{a}_1, \mathbf{a}_2, \dots, \mathbf{a}_M]$, and let $\mathbf{b} = \text{vec}(\boldsymbol{\Gamma}^T)$ and $\mathcal{S}_i = \{i_1, i_2, \dots, i_{|\mathcal{S}_i|}\}$. Then

$$\|\mathbf{B} \mathbf{M} - \boldsymbol{\Gamma}\|_F^2 = \|\mathbf{A} \mathbf{x} - \mathbf{b}\|_2^2,$$

where

$$\mathbf{A} = \begin{bmatrix} \mathbf{A}_{11} & \mathbf{A}_{12} & \cdots & \mathbf{A}_{1M} \\ \mathbf{A}_{21} & \mathbf{A}_{22} & \cdots & \mathbf{A}_{2M} \\ \vdots & \vdots & \ddots & \vdots \\ \mathbf{A}_{M1} & \mathbf{A}_{M2} & \cdots & \mathbf{A}_{MM} \end{bmatrix} \in \mathbb{R}^{2MK \times \sum_{i=1}^M |\mathcal{S}_i|}$$

with $\mathbf{A}_{ij} \in \mathbb{R}^{2K \times |\mathcal{S}_i|}$ given by

$$\mathbf{A}_{ij}(:, q) = \begin{cases} \mathbf{a}_{j_q}, & \text{if } i = j; \\ \mathbf{a}_j, & \text{if } i = j_q; \\ \mathbf{0}, & \text{otherwise,} \end{cases} \quad q = 1, 2, \dots, |\mathcal{S}_i|; \quad (19)$$

here $\mathbf{A}_{ij}(:, q)$ denotes the q -th column of \mathbf{A}_{ij} . With the above notations, problem (17) can be written as

$$\min_{\mathbf{x}} \|\mathbf{A} \mathbf{x} - \mathbf{b}\|_2^2 + \frac{\xi}{2} \|\mathbf{x} - \mathbf{x}^t\|_2^2,$$

which admits a closed form solution as

$$\mathbf{x}^{t+1} = (\mathbf{A}^T \mathbf{A} + \xi \mathbf{I})^{-1} (\mathbf{A}^T \mathbf{b} + \xi \mathbf{x}^t). \quad (20)$$

Note that calculating (20) becomes computationally expensive when the number of columns in \mathbf{A} is large. This happens, e.g., for fully-connected RIS, in which case the number of columns in \mathbf{A} is $M(M+1)/2$, resulting in a complexity of $\mathcal{O}(M^6)$ for calculating the matrix inversion in (20). To address this issue, we adopt an equivalent expression for (20) when the number of columns in \mathbf{A} exceeds the number of its rows, i.e., when $\sum_{i=1}^M |\mathcal{S}_i| \geq 2MK$, as follows:

$$\mathbf{x}^{t+1} = \frac{1}{\xi} \left(\mathbf{I} - \mathbf{A}^T (\mathbf{A} \mathbf{A}^T + \xi \mathbf{I})^{-1} \mathbf{A} \right) (\mathbf{A}^T \mathbf{b} + \xi \mathbf{x}^t). \quad (21)$$

With (21), we only need to compute a matrix inversion of dimension $2MK$ rather than $\sum_{i=1}^M |\mathcal{S}_i|$.

After obtaining \mathbf{x}^{t+1} , we update \mathbf{B}^{t+1} according to the relationship between \mathbf{x} and \mathbf{B} defined in (18). Specifically, \mathbf{B}^{t+1} is given by

$$B_{i,j}^{t+1} = \begin{cases} \mathbf{x}^{t+1}(\sum_{q=1}^{i-1} |\mathcal{S}_q| + l), & \text{if } j = i_i; \\ \mathbf{x}^{t+1}(\sum_{q=1}^{j-1} |\mathcal{S}_q| + l), & \text{if } i = j_i; \\ 0, & \text{otherwise,} \end{cases}$$

where we use the notation $\mathbf{x}(S)$ to denote a sub-vector of \mathbf{x} consisting of elements indexed by S .

We remark here that the proximal term in (11d) is introduced to ensure that the problem is strongly convex (and thus admits a unique solution), which is essential for the convergence of the algorithm. In addition, it serves as a safeguard to avoid the elements in \mathbf{x} (equivalently in \mathbf{B}) becoming excessively large. Without the proximal term, the elements in \mathbf{x} would take on large values when there are small singular values of \mathbf{A} , leading to unstable performance.

5) *Update of \mathbf{U}* : The \mathbf{U} -subproblem (11e) is separable in $\{\mathbf{u}_k\}_{1 \leq k \leq K}$. For each \mathbf{u}_k , the problem is an unconstrained convex quadratic programming, with the closed-form solution given by

$$\begin{aligned} \mathbf{u}_k^{t+1} = & \left((1 + \gamma_k^{t+1}) |y_k^{t+1}|^2 \mathbf{G} \mathbf{W}^{t+1} (\mathbf{W}^{t+1})^\dagger \mathbf{G}^\dagger \right. \\ & + \frac{\rho}{2} (\mathbf{I} + Z_0^2 (\mathbf{B}^{t+1})^2) \left. \right)^{-1} \left((1 + \gamma_k^{t+1}) (y_k^{t+1})^\dagger \mathbf{G} \mathbf{w}_k^{t+1} \right. \\ & \left. - \frac{1}{2} (\mathbf{I} + i Z_0 \mathbf{B}^{t+1}) \boldsymbol{\lambda}_k^t + \frac{\rho}{2} (\mathbf{I} + i Z_0 \mathbf{B}^{t+1})^2 \mathbf{h}_k \right), \end{aligned}$$

where we have used the fact that $(\mathbf{I} - i Z_0 \mathbf{B})^\dagger = \mathbf{I} + i Z_0 \mathbf{B}$, and $\boldsymbol{\lambda}_k$ denotes the k -th column of $\boldsymbol{\lambda}$.

C. Complexity and Convergence Analysis

In this subsection, we give complexity and convergence analysis of the proposed pp-ADMM algorithm.

1) *Complexity Analysis*: The complexity of updating variables \mathbf{y} and $\boldsymbol{\gamma}$ is $\mathcal{O}(MNK + K^2)$. Updating variable \mathbf{W} requires a complexity of $\mathcal{O}(N^2K + N^3)$, where the first term comes from constructing \mathbf{Q} (note that $\mathbf{G}^\dagger \mathbf{U}^t$ has already been calculated via the update of \mathbf{y} and $\boldsymbol{\gamma}$), and the second term comes from calculating the eigenvalue decomposition of \mathbf{Q} . The computational cost of updating variable \mathbf{B} is dominated by calculating the matrix inversion in (20) or (21), whose complexity is $\mathcal{O}((\min\{\sum_{i=1}^M |\mathcal{S}_i|, 2MK\})^3)$. The complexity of updating variable \mathbf{U} is $\mathcal{O}(M^3K + MNK)$. Finally, updating $\boldsymbol{\lambda}$ requires a complexity of $\mathcal{O}(M^2K)$. Since in practice the number of RIS elements M is much larger than the number of transmit antennas N and the number of users K , the total per-iteration complexity of the proposed pp-ADMM algorithm is $\mathcal{O}(M^3K + (\min\{\sum_{i=1}^M |\mathcal{S}_i|, 2MK\})^3)$.

2) *Convergence Analysis*: Classical convergence results for ADMM-type algorithms are typically established for optimization problems with linear constraints [40]. In our work, however, ADMM is applied to tackle the bi-linear constraint in (7b). Although a few works have also studied the convergence of ADMM on bi-linear constrained problems [42], [43], the problems considered therein are much simpler than (9). Fortunately, by leveraging the special structure of the bilinear constraint (7b), we can establish the convergence of our proposed pp-ADMM algorithm.

Theorem 1. *Assume that the sequences $\{\mathbf{U}^t\}_{t \geq 0}$ and $\{\boldsymbol{\lambda}^t\}_{t \geq 0}$ generated by the pp-ADMM algorithm in (11) are bounded. Then there exists $\rho_0 > 0$ such that when $\rho > \rho_0$, any limit point $(\mathbf{y}^*, \boldsymbol{\gamma}^*, \mathbf{W}^*, \mathbf{B}^*, \mathbf{U}^*)$ of $(\mathbf{y}^t, \boldsymbol{\gamma}^t, \mathbf{W}^t, \mathbf{B}^t, \mathbf{U}^t)$ is a stationary point of problem (9).*

Proof. See Appendix B. \square

We remark here that the assumption on the boundedness of the sequences $\{\mathbf{U}^t\}_{t \geq 0}$ and $\{\boldsymbol{\lambda}^t\}_{t \geq 0}$ are imposed for technical reasons. Nevertheless, numerous simulation results show that it is always satisfied.

IV. TRANSMIT POWER MINIMIZATION PROBLEM

In this section, we investigate the transmit power minimization problem in (5).

A. An Equivalent Formulation

Similar to Section III-A, we introduce an auxiliary variable $\mathbf{U} = \boldsymbol{\Theta}^\dagger \mathbf{H}$ to deal with the matrix inversion in constraint (5c), which yields

$$\min_{\mathbf{W}, \mathbf{B}, \mathbf{U}} \|\mathbf{W}\|_F^2 \quad (22a)$$

$$\text{s.t. } \text{SINR}_k(\mathbf{u}_k, \mathbf{W}) \geq \Gamma_k, \quad k = 1, 2, \dots, K, \quad (22b)$$

$$(\mathbf{I} - i Z_0 \mathbf{B}) \mathbf{U} = (\mathbf{I} + i Z_0 \mathbf{B}) \mathbf{H}, \quad (22c)$$

$$\mathbf{B} = \mathbf{B}^T, \quad \mathbf{B} \in \mathcal{B}. \quad (22d)$$

To tackle the QoS constraint in (22b), we introduce another auxiliary variable $\mathbf{Y} = \mathbf{U}^\dagger \mathbf{G} \mathbf{W} \in \mathbb{C}^{K \times K}$. Then problem (22) can be transformed into the following equivalent form:

$$\min_{\mathbf{W}, \mathbf{B}, \mathbf{U}, \mathbf{Y}} \|\mathbf{W}\|_F^2 \quad (23a)$$

$$\text{s.t. } Y_{k,k} \geq \sqrt{\Gamma_k (\sum_{j \neq k} |Y_{k,j}|^2 + \sigma^2)}, \quad k = 1, 2, \dots, K, \quad (23b)$$

$$\mathcal{I}(Y_{k,k}) = 0, \quad k = 1, 2, \dots, K, \quad (23c)$$

$$\mathbf{Y} = \mathbf{U}^\dagger \mathbf{G} \mathbf{W}, \quad (23d)$$

$$(22c) \text{ and } (22d). \quad (23e)$$

Note that in (23), the non-convex QoS constraint

$$|Y_{k,k}|^2 \geq \Gamma_k (\sum_{j \neq k} |Y_{k,j}|^2 + \sigma^2), \quad k = 1, 2, \dots, K \quad (24)$$

has been replaced by the convex constraints in (23b) and (23c), where (23b) can be formulated as a second-order cone (SOC) constraint. The rationale behind this is that, given any feasible pair (\mathbf{W}, \mathbf{Y}) satisfying (23d) and (24), we can rotate $\{\mathbf{w}_k\}_{1 \leq k \leq K}$ to obtain a new feasible pair $(\bar{\mathbf{W}}, \bar{\mathbf{Y}})$ such that $\{\bar{Y}_{k,k}\}_{1 \leq k \leq K}$ is nonnegative (i.e., $(\bar{\mathbf{W}}, \bar{\mathbf{Y}})$ satisfy (23b)–(23d)) and the objective value remains the same. This idea is inspired by the classical work [36], in which a similar transformation was applied to reformulate the traditional power minimization problem as an SOCP.

Now, the complicated QoS constraint in (22b) has been reformulated as a bilinear constraint (23d) and two simple constraints, (23b) and (23c), on \mathbf{Y} that allow for efficient projection. To be more specific, the projection onto set

$$\mathcal{Y} := \{\mathbf{Y} \in \mathbb{C}^{K \times K} \mid \mathbf{Y} \text{ satisfies (23b) and (23c)}\}$$

can be efficiently computed by solving K one-dimensional quartic equations; see further details below.

B. pp-ADMM Algorithm for Solving (23)

Problem (23) has a simple objective function with separable constraints on \mathbf{Y} and \mathbf{B} , as well as two bilinear constraints that couple variables $(\mathbf{B}, \mathbf{U}, \mathbf{W})$, which is suitable to be solved via an ADMM framework. Next, we custom-build an efficient pp-ADMM algorithm for solving (23).

First, the augmented Lagrangian function of (23) is given by

$$\begin{aligned} \mathcal{L}_\rho(\mathbf{Y}, \mathbf{W}, \mathbf{B}, \mathbf{U}, \boldsymbol{\lambda}, \boldsymbol{\mu}) &= \|\mathbf{W}\|_F^2 + \langle \boldsymbol{\lambda}, (\mathbf{I} - i Z_0 \mathbf{B}) \mathbf{U} - (\mathbf{I} + i Z_0 \mathbf{B}) \mathbf{H} \rangle \\ &+ \frac{\rho \lambda}{2} \|(\mathbf{I} - i Z_0 \mathbf{B}) \mathbf{U} - (\mathbf{I} + i Z_0 \mathbf{B}) \mathbf{H}\|_F^2 \\ &+ \langle \boldsymbol{\mu}, \mathbf{Y} - \mathbf{U}^\dagger \mathbf{G} \mathbf{W} \rangle + \frac{\rho \mu}{2} \|\mathbf{Y} - \mathbf{U}^\dagger \mathbf{G} \mathbf{W}\|_F^2, \end{aligned} \quad (25)$$

where $(\boldsymbol{\lambda}, \boldsymbol{\mu})$ are the Lagrange multipliers associated with the bilinear constraints (22c) and (23d), respectively, and $\boldsymbol{\rho} = (\rho_\lambda, \rho_\mu)$ are the corresponding penalty parameters.

Our proposed pp-ADMM algorithm is given below.

$$\mathbf{Y}^{t+1} \in \arg \min_{\mathbf{Y} \in \mathcal{Y}} \mathcal{L}_\rho(\mathbf{Y}, \mathbf{W}^t, \mathbf{B}^t, \mathbf{U}^t, \boldsymbol{\lambda}^t, \boldsymbol{\mu}^t), \quad (26a)$$

$$\mathbf{W}^{t+1} \in \arg \min \mathcal{L}_\rho(\mathbf{Y}^{t+1}, \mathbf{W}, \mathbf{B}^t, \mathbf{U}^t, \boldsymbol{\lambda}^t, \boldsymbol{\mu}^t), \quad (26b)$$

$$\mathbf{B}^{t+1} \in \arg \min_{\substack{\mathbf{B} = \mathbf{B}^T \\ \mathbf{B} \in \mathcal{B}}} \mathcal{L}_\rho(\mathbf{Y}^{t+1}, \mathbf{W}^{t+1}, \mathbf{B}, \mathbf{U}^t, \boldsymbol{\lambda}^t, \boldsymbol{\mu}^t) + \frac{\xi}{2} \|\mathbf{B} - \mathbf{B}^t\|_F^2, \quad (26c)$$

$$\mathbf{U}^{t+1} \in \arg \min \mathcal{L}_\rho(\mathbf{Y}^{t+1}, \mathbf{W}^{t+1}, \mathbf{B}^{t+1}, \mathbf{U}, \boldsymbol{\lambda}^t, \boldsymbol{\mu}^t), \quad (26d)$$

$$\boldsymbol{\lambda}^{t+1} = \boldsymbol{\lambda}^t + \rho_\lambda ((\mathbf{I} - iZ_0 \mathbf{B}^{t+1}) \mathbf{U}^{t+1} - (\mathbf{I} + iZ_0 \mathbf{B}^{t+1}) \mathbf{H}), \quad (26e)$$

$$\boldsymbol{\mu}^{t+1} = \boldsymbol{\mu}^t + \rho_\mu (\mathbf{Y}^{t+1} - (\mathbf{U}^{t+1})^\dagger \mathbf{G} \mathbf{W}^{t+1}). \quad (26f)$$

The only difference between the above algorithm and classical ADMM is an extra proximal term for updating \mathbf{B} , which is introduced to ensure the stability and convergence of the algorithm, as discussed in Section III-B. The update of \mathbf{B} follows exactly the same procedure as in (16). In addition, the \mathbf{W} - and \mathbf{U} -subproblems in (26b) and (26d) are both unconstrained convex quadratic programming, which admit closed-form solutions. We omit the details for brevity. Next, we discuss the solution of the \mathbf{Y} -subproblem (26a).

According to (25) and (26a), the \mathbf{Y} -subproblem is to compute the projection of $(\mathbf{U}^t)^\dagger \mathbf{G} \mathbf{W}^t - \boldsymbol{\mu}^t / \rho_\mu$ onto set \mathcal{Y} . Since constraint (23b) is separable across the rows of \mathbf{Y} , the \mathbf{Y} -subproblem can be divided into K independent problems as follows (where $k = 1, 2, \dots, K$):

$$\begin{aligned} \min_{\mathbf{Y}_{k,:}} \sum_{j=1}^K \left| Y_{k,j} - (\mathbf{u}_k^t)^\dagger \mathbf{G} \mathbf{w}_j^t + \frac{\mu_{k,j}^t}{\rho_\mu} \right|^2 \\ \text{s.t. } Y_{k,k} \geq \sqrt{\Gamma_k (\sum_{j \neq k} |Y_{k,j}|^2 + \sigma^2)}, \quad \mathcal{I}(Y_{k,k}) = 0. \end{aligned} \quad (27)$$

Clearly, the constraint in (27) depends only on the magnitude of $\{Y_{k,j}\}_{j \neq k}$ and is irrelevant to their phases. To minimize the objective function, the phase of $Y_{k,j}$ should align with that of $(\mathbf{u}_k^t)^\dagger \mathbf{G} \mathbf{w}_j^t - \mu_{k,j}^t / \rho_\mu$, where $j \neq k$. Due to this, and by further squaring the constraint and noting that $Y_{k,k}$ is real-valued and positive, we can rewrite problem (27) into the following equivalent form:

$$\begin{aligned} \min_{\{r_{k,j}\}_{j=1}^K} \sum_{j=1}^K (r_{k,j} - a_{k,j})^2 \\ \text{s.t. } r_{k,k}^2 \geq \Gamma_k (\sum_{j \neq k} r_{k,j}^2 + \sigma^2), \quad r_{k,k} \geq 0. \end{aligned} \quad (28)$$

where

$$r_{k,j} = \begin{cases} |Y_{k,j}|, & \text{if } j \neq k; \\ Y_{k,k}, & \text{if } j = k, \end{cases}$$

and

$$a_{k,j} = \begin{cases} |(\mathbf{u}_k^t)^\dagger \mathbf{G} \mathbf{w}_j^t - \mu_{k,j}^t / \rho_\mu|, & \text{if } j \neq k; \\ \mathcal{R}((\mathbf{u}_k^t)^\dagger \mathbf{G} \mathbf{w}_k^t - \mu_{k,k}^t / \rho_\mu), & \text{if } j = k. \end{cases}$$

Strictly speaking, there should be nonnegative constraints on $\{r_{k,j}\}_{j \neq k}$ in (28), as they represent the magnitudes of $\{Y_{k,j}\}_{j \neq k}$. However, we can ignore these constraints since

the optimal solution to (28) will naturally be nonnegative due to the nonnegativity of $\{a_{k,j}\}_{j \neq k}$. By analyzing the KKT condition of (28), we claim that the optimal solution to (28) is given by

$$r_{k,j}^* = \begin{cases} \left(\Gamma_k \sum_{j \neq k} \frac{a_{k,j}^2}{(1 + \Gamma_k)^2} + \Gamma_k \sigma^2 \right)^{1/2}, & \text{if } j = k \text{ and } a_{k,k} = 0; \\ \frac{a_{k,j}}{1 - \eta}, & \text{if } j = k \text{ and } a_{k,k} \neq 0; \\ \frac{a_{k,j}}{1 + \Gamma_k \eta}, & \text{if } j \neq k, \end{cases} \quad (29)$$

where

$$\eta = \begin{cases} 0, & \text{if } a_{k,k} \geq (\Gamma_k \sum_{j \neq k} a_{k,j}^2 + \Gamma_k \sigma^2)^{1/2}; \\ \eta_1^*, & \text{if } 0 < a_{k,k} < (\Gamma_k \sum_{j \neq k} a_{k,j}^2 + \Gamma_k \sigma^2)^{1/2}; \\ 1, & \text{if } a_{k,k} = 0; \\ \eta_2^*, & \text{if } a_{k,k} < 0, \end{cases} \quad (30)$$

with $\eta_1^* \in (0, 1)$ and $\eta_2^* \in (1, \infty)$ being the unique roots of the following equation in the intervals $(0, 1)$ and $(1, \infty)$, respectively:

$$\frac{\Gamma_k \sum_{j \neq k} a_{k,j}^2}{(1 + \Gamma_k \eta)^2} - \frac{a_{k,k}^2}{(1 - \eta)^2} + \Gamma_k \sigma^2 = 0. \quad (31)$$

A rigorous proof of (29) is given in Appendix A. Eq. (31) can be further transformed into a quartic equation and solved in closed-form. Combining the above, we get

$$Y_{k,j}^{t+1} = \begin{cases} r_{k,j}^* e^{i \arg((\mathbf{u}_k^t)^\dagger \mathbf{G} \mathbf{w}_j^t - \mu_{k,j}^t / \rho_\mu)}, & \text{if } j \neq k; \\ r_{k,k}^*, & \text{if } j = k. \end{cases}$$

C. Complexity and Convergence Analysis

We next give complexity and convergence analysis of the above algorithm.

1) *Complexity Analysis*: The complexity for updating variables \mathbf{Y} , \mathbf{W} , \mathbf{B} , \mathbf{U} , $\boldsymbol{\lambda}$, and $\boldsymbol{\mu}$ are $\mathcal{O}(K^2)$, $\mathcal{O}(N^2 K + NK^2 + N^3)$, $\mathcal{O}((\min\{\sum_{i=1}^M |S_i|, 2MK\})^3)$, $\mathcal{O}(M^3 + M^2 K + MNK + MK^2)$, $\mathcal{O}(M^2 K)$, and $\mathcal{O}(MNK)$, respectively⁵. To conclude, the total per-iteration complexity of the pp-ADMM algorithm in (26) is $\mathcal{O}(M^3 + (\min\{\sum_{i=1}^M |S_i|, 2MK\})^3)$.

2) *Convergence Analysis*: Similar to Theorem 1, we can establish the convergence of the pp-ADMM algorithm in (26).

Theorem 2. Assume that

- The sequences $\{\mathbf{W}^t\}_{t \geq 0}$, $\{\mathbf{U}^t\}_{t \geq 0}$, $\{\boldsymbol{\lambda}^t\}_{t \geq 0}$, and $\{\boldsymbol{\mu}^t\}_{t \geq 0}$ generated by the pp-ADMM algorithm in (26) are bounded.
- The minimum singular value of $\{\mathbf{G}^\dagger \mathbf{U}^t\}_{t \geq 0}$ has a uniformly positive lower bound.

Then there exists $c_0 > 0$ and $\rho_0 > 0$ such that when $\rho_\lambda > c_0 \rho_\mu > \rho_0$, any limit point $(\mathbf{Y}^*, \mathbf{W}^*, \mathbf{B}^*, \mathbf{U}^*)$ of $(\mathbf{Y}^t, \mathbf{W}^t, \mathbf{B}^t, \mathbf{U}^t)$ is a stationary point of problem (23).

⁵We remark that the complexity of calculating $(\mathbf{U}^t)^\dagger \mathbf{G} \mathbf{W}^t$ is not included in the complexity of updating \mathbf{Y}^{t+1} , as this computation has already been performed in updating $\boldsymbol{\mu}^t$. Similarly, the complexity of calculating $\mathbf{G}^\dagger \mathbf{U}^t$ is excluded from the complexity of updating \mathbf{W}^{t+1} .

Proof. See Appendix C. \square

Remark 1. It is worth mentioning a related work [31], in which a penalty dual decomposition (PDD)-based optimization framework was developed to solve both sum-rate maximization and transmit power minimization problems for BD-RIS-aided MU-MISO communication systems. Our proposed approach outperforms [31] in that it is applicable to any BD-RIS architecture, while the framework in [31] is limited to only fully- and group-connected architectures. Moreover, compared to the PDD algorithm in [31], our proposed pp-ADMM algorithms are significantly more computationally efficient. The reasons are as follows. First, the PDD algorithm in [31] is double loop, where an inner loop is required to tackle the symmetric and unitary constraints on the scattering matrix, whereas the proposed pp-ADMM framework is single-loop. Second, in the PDD algorithm, the complexity of updating the scattering matrix scales with M^6 [31, Eq. (59)] at each iteration, while our approach reduces this to K^3M^3 by leveraging (21). Finally, for the transmit power minimization problem, the PDD algorithm formulates a SOCP in each inner iteration to deal with the QoS constraint, which is solved by directly calling CVX, resulting in a high computational cost. In contrast, our proposed approach introduces appropriate auxiliary variables to simplify the QoS constraint, allowing for closed-form updates in each iteration.

V. GENERALIZATIONS

In previous sections, we focus on sum-rate maximization and transmit power minimization problems for MU-MISO systems. However, the technique for dealing with BD-RIS-related variables (i.e., Θ and \mathbf{B}) is general, and the proposed optimization framework can be extended to other utility functions and MU-MIMO systems. In this section, we explore the broader applicability of our proposed approach.

A. General Utility Functions

Consider a utility optimization problem in the following form:

$$\begin{aligned} \max_{\Theta, \mathbf{W}} \quad & F(\{\text{SINR}_k(\Theta, \mathbf{W})\}_{k=1}^K) \\ \text{s.t.} \quad & \Theta = (\mathbf{I} + iZ_0\mathbf{B})^{-1} (\mathbf{I} - iZ_0\mathbf{B}), \\ & \mathbf{B} = \mathbf{B}^T, \mathbf{B} \in \mathcal{B}, \\ & \mathbf{W} \in \mathcal{W}, \end{aligned} \quad (32)$$

where $F(\{\text{SINR}_k(\Theta, \mathbf{W})\}_{k=1}^K)$ is a general utility function and $\mathbf{W} \in \mathcal{W}$ represents the constraint imposed on the transmitter side (e.g., the transmit power constraint). The above model encompasses the sum-rate maximization problem in (4) with

$$F(\{\text{SINR}_k(\Theta, \mathbf{W})\}_{k=1}^K) = \sum_{k=1}^K \log_2(1 + \text{SINR}_k(\Theta, \mathbf{W}))$$

and $\mathcal{W} = \{\|\mathbf{W}\|_F^2 \leq P_T\}$, and the transmit power minimization problem in (5) with

$$\begin{aligned} & F(\{\text{SINR}_k(\Theta, \mathbf{W})\}_{k=1}^K) \\ & = -\|\mathbf{W}\|_F^2 - \sum_{k=1}^K \mathbb{I}_{\{\text{SINR}_k(\Theta, \mathbf{W}) \geq \gamma_k\}}(\Theta, \mathbf{W}) \end{aligned}$$

and $\mathcal{W} = \mathbb{C}^{N \times K}$, where $\mathbb{I}_{\mathcal{X}}(x)$ refers to the indicator function of set \mathcal{X} , defined as $\mathbb{I}_{\mathcal{X}}(x) = 0$ if $x \in \mathcal{X}$, and $\mathbb{I}_{\mathcal{X}}(x) = \infty$ otherwise.

Inspired by the previous sections, we extract the following procedures for solving (32).

Step 1: The first step deals with the difficulties introduced by BD-RIS. Specifically, we introduce auxiliary variables $\mathbf{u}_k = \Theta^\dagger \mathbf{h}_k$, $k = 1, 2, \dots, K$, to transform (32) into the following more tractable form:

$$\max_{\mathbf{U}, \mathbf{W}} F(\{\text{SINR}_k(\mathbf{u}_k, \mathbf{W})\}_{k=1}^K) \quad (33a)$$

$$\text{s.t.} \quad (\mathbf{I} - iZ_0\mathbf{B})\mathbf{U} = (\mathbf{I} + iZ_0\mathbf{B})\mathbf{H}, \quad (33b)$$

$$\mathbf{B} = \mathbf{B}^T, \mathbf{B} \in \mathcal{B}, \quad (33c)$$

$$\mathbf{W} \in \mathcal{W}, \quad (33d)$$

where $\text{SINR}_k(\mathbf{u}_k, \mathbf{W})$ is given in (6). This transformation is the key of our proposed framework, which offers a simpler formulation with reduced dimensionality; see the discussions below (7).

Step 2: The second step is to further simplify the objective function in (33a), typically by introducing appropriate auxiliary variables. The approach for this step relies on the specific structure of the utility function under consideration. For example, fractional programming is employed to simplify the sum-rate objective function in (8), and an auxiliary variable $\mathbf{Y} = \mathbf{U}^\dagger \mathbf{G} \mathbf{W}$ is introduced in (23) to simplify the QoS requirement.

Step 3: The final step is to employ an ADMM framework to deal with the bilinear constraint (33b). In particular, appropriate proximal terms can be introduced for specific variables to ensure the convergence of the proposed algorithm. For efficient implementation, the objective function formulated in Step 2 should be simple with respect to each variable block.

In addition to the sum-rate maximization and transmit power minimization problems considered in the previous sections, we next briefly discuss the application of the above framework to two other widely used utilities: max-min fairness and energy efficiency maximization.

1) Max-min fairness: Max-min fairness aims to maximize the utility of the user with the worst performance. Mathematically, the utility function is given by

$$F(\{\text{SINR}_k(\mathbf{u}_k, \mathbf{W})\}_{k=1}^K) = \min_k \text{SINR}_k(\mathbf{u}_k, \mathbf{W}).$$

Introducing an auxiliary variable $\Gamma = \min_k \text{SINR}_k(\mathbf{u}_k, \mathbf{W})$ and employing the transformation in Step 1, the max-min fairness model can be written as

$$\begin{aligned} \max_{\mathbf{U}, \mathbf{W}, \Gamma} \quad & \Gamma \\ \text{s.t.} \quad & \text{SINR}_k(\mathbf{u}_k, \mathbf{W}) \geq \Gamma, \quad k = 1, 2, \dots, K, \\ & (\mathbf{I} - iZ_0\mathbf{B})\mathbf{U} = (\mathbf{I} + iZ_0\mathbf{B})\mathbf{H}, \\ & \mathbf{B} = \mathbf{B}^T, \mathbf{B} \in \mathcal{B}, \\ & \|\mathbf{W}\|_F^2 \leq P_T, \end{aligned} \quad (34)$$

where we consider the total transmit power constraint at the BS, i.e., $\mathcal{W} = \{\mathbf{W} \mid \|\mathbf{W}\|_F^2 \leq P_T\}$. The above model is similar to (23), but with the following two differences. First, the total transmit power is imposed as a constraint in (34), while it appears as the objective function in (23). Second, the SINR threshold Γ in (34) is treated as a variable, while $\{\Gamma_k\}_{k=1}^K$ in (23) are fixed problem parameters. As in (23), we further simplify the QoS constraint with an auxiliary variable $\mathbf{Y} = \mathbf{U}^\dagger \mathbf{G} \mathbf{W}$, after which an ADMM framework similar to (26) can be employed to solve the problem. In particular, following the procedure of ADMM, the only additional variable Γ is updated as

$$\Gamma^{t+1} = \min_k \left\{ \frac{|Y_{k,k}^t|^2}{\sum_{j \neq k} |Y_{k,j}^t|^2 + \sigma^2} \right\}$$

in each iteration.

2) *Energy efficiency maximization*: The energy efficiency of the system is given as

$$F(\{\text{SINR}_k(\mathbf{u}_k, \mathbf{W})\}_{k=1}^K) = \frac{\sum_{k=1}^K \log(1 + \text{SINR}_k(\mathbf{u}_k, \mathbf{W}))}{\mu_0 \|\mathbf{W}\|_F^2 + P_c},$$

where μ_0 is the power amplifier efficiency and P_c represents the total circuit power. Applying the fractional programming technique [38] and the transformation in Step 1, the energy efficiency maximization problem can be equivalently formulated as

$$\begin{aligned} \max_{\mathbf{U}, \mathbf{W}, Y} \quad & 2Y \sum_{k=1}^K \log(1 + \text{SINR}_k(\mathbf{u}_k, \mathbf{W})) - Y^2 (\mu_0 \|\mathbf{W}\|_F^2 + P_c)^2 \\ \text{s.t.} \quad & (\mathbf{I} - iZ_0 \mathbf{B}) \mathbf{U} = (\mathbf{I} + iZ_0 \mathbf{B}) \mathbf{H}, \\ & \mathbf{B} = \mathbf{B}^T, \mathbf{B} \in \mathcal{B}, \\ & \|\mathbf{W}\|_F^2 \leq P_T, \end{aligned}$$

where we consider the total transmit power constraint at the BS. The sum-rate expression in the objective function can further be simplified as in (8), enabling the application of an efficient ADMM framework. The corresponding algorithm differs from (11) mainly in the formula of the \mathbf{W} -subproblem and the inclusion of an additional variable Y . Specifically, the \mathbf{W} -subproblem has a quartic objective function and a quadratic transmit power constraint, which is different from the QCQP in (11c). Nonetheless, it can still be efficiently solved using a bisection search. We omit the details for brevity. The variable Y is updated in closed-form at each iteration as

$$Y^{t+1} = \frac{\tilde{R}(\mathbf{y}^t, \boldsymbol{\gamma}^t, \mathbf{W}^t, \mathbf{U}^t)}{(\mu_0 \|\mathbf{W}\|_F^2 + P_c)^2},$$

where $\tilde{R}(\mathbf{y}, \boldsymbol{\gamma}, \mathbf{W}, \mathbf{U})$ is given in (8).

B. MU-MIMO Systems

The proposed framework can also be extended to MU-MIMO systems. Denote $\mathbf{H}_k \in \mathbb{C}^{N_k \times M}$ as the channel from BD-RIS to the k -th user, where N_k represents the number of antennas at the k -th user. In addition, let $\mathbf{s}_k \in \mathbb{C}^{d_k}$ be the data streams intended for the k -th user, and let $\mathbf{W}_k \in \mathbb{C}^{N \times d_k}$ denote the corresponding beamforming matrix. The performance

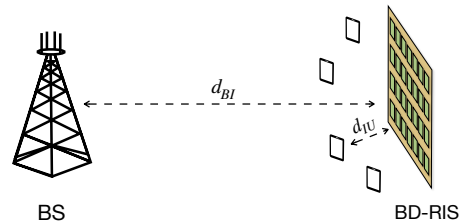


Fig. 2. An illustration of the BD-RIS aided MU-MISO system for simulation.

of the k -th user is typically characterized by its achievable rate, given by

$$R_k = \log \det \left(\mathbf{I} + \mathbf{H}_{k,\text{eff}} \mathbf{W}_k \mathbf{W}_k^\dagger \mathbf{H}_{k,\text{eff}}^\dagger \right. \\ \left. \times \left(\sum_{j \neq k} \mathbf{H}_{k,\text{eff}} \mathbf{W}_j \mathbf{W}_j^\dagger \mathbf{H}_{k,\text{eff}}^\dagger + \sigma^2 \mathbf{I} \right)^{-1} \right),$$

where $\mathbf{H}_{k,\text{eff}} := \mathbf{H}_k \boldsymbol{\Theta} \mathbf{G} \in \mathbb{C}^{N_k \times N}$ represents the effective channel from the BS to user k . Following a similar technique as in the MU-MISO case, we introduce auxiliary variables

$$\mathbf{U}_k = (\mathbf{H}_k \boldsymbol{\Theta})^\dagger \in \mathbb{C}^{M \times N_k}, \quad k = 1, 2, \dots, K, \quad (35)$$

with which the effective channel can be written as $\mathbf{H}_{\text{eff},k} = \mathbf{U}_k^\dagger \mathbf{G}$, and the constraint $\boldsymbol{\Theta} = (\mathbf{I} + iZ_0 \mathbf{B})^{-1} (\mathbf{I} - iZ_0 \mathbf{B})$ is transformed into

$$(\mathbf{I} - iZ_0 \mathbf{B}) \mathbf{U}_k = (\mathbf{I} + iZ_0 \mathbf{B}) \mathbf{H}_k^\dagger, \quad k = 1, 2, \dots, K. \quad (36)$$

The difference from the MU-MISO case is that the auxiliary variable introduced for each user, i.e., \mathbf{U}_k , is now a matrix rather than a vector, due to the presence of multiple antennas at the user side. Nevertheless, \mathbf{U}_k remains related to \mathbf{B} through a bilinear constraint as shown in (36), which can still be tackled using an ADMM framework. For example, the sum-rate maximization problem for MU-MIMO systems can be solved by first applying fractional programming technique (in matrix form) [44] to simplify the objective function and then employing a similar pp-ADMM algorithm as in (11).

VI. SIMULATION RESULTS

In this section, we present simulation results to demonstrate the effectiveness of the proposed algorithms and evaluate the performance of various BD-RIS architectures.

In our simulation, we adopt the same setup as in [7]. Specifically, we consider a BD-RIS aided MU-MISO system as shown in Fig. 2, where the distance between the BS and the BD-RIS is $d_{BI} = 50$ m, and K users are randomly located near the BD-RIS with the same distance $d_{IU} = 2.5$ m. Unless otherwise stated, the number of antennas at the BS is $N = 4$, and the number of users is $K = 4$. The channels from the BS to the BD-RIS and from the BD-RIS to the users are modeled with both large-scale fading and small-scale fading. For large-scale fading, we use the distance-dependent path loss $\zeta(d) = \eta_0 d^{-\alpha}$, where ζ_0 represents the signal attenuation at a reference distance $d_0 = 1$ m, which is set as $\zeta_0 = -30$ dB, and α is the path-loss exponent, which is set as $\alpha = 2.2$ for both the channel from the BS to the BD-RIS and the channel from

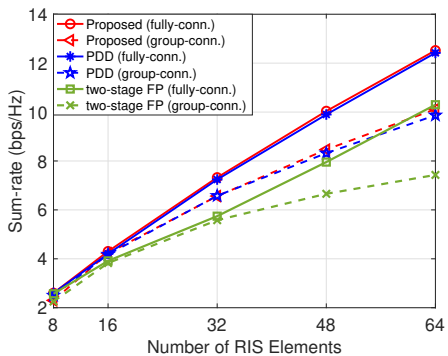


Fig. 3. Sum-rate versus number of RIS elements ($N = K = 4, G_s = 4$).

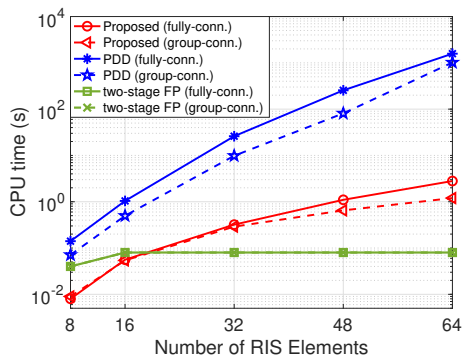


Fig. 4. CPU time versus number of RIS elements for sum-rate maximization ($N = K = 4, G_s = 4$).

the BD-RIS to the users. The small-scale fading is modeled as Rician fading with a Rician factor of $\kappa = 2$ dB for both channels. The noise power is set as $\sigma^2 = -80$ dBm.

We first evaluate the effectiveness of the proposed pp-ADMM algorithms by comparing them with the state-of-the-art approaches. Since no existing algorithm is applicable to general BD-RIS architectures, we focus on fully- and group-connected BD-RIS architectures, where the group size is set as $G_s = 4$. For the sum-rate maximization problem, we include the PDD algorithm in [31] and the two-stage FP algorithm in [29] as benchmarks. For the transmit power minimization problem, we include the PDD algorithm in [31] as a benchmark, which, to the best of our knowledge, is the only existing algorithm for solving the transmit power minimization problem in the BD-RIS literature.

Figs. 3 and 4 present the simulation results for the sum-rate maximization problem, where Fig. 3 shows the sum-rate achieved by different algorithms, and Fig. 4 illustrates their CPU times. As shown in the figures, the proposed pp-ADMM algorithm achieves a similar sum-rate performance compared to PDD with a significantly reduced CPU time. Both of these two approaches yield a substantially higher sum-rate than the two-stage FP algorithm in [29]. The superiority is particularly prominent when the number of RIS elements is large, in which cases a 20% gain can be observed. Nevertheless, the two-stage FP algorithm is the most computationally efficient, whose computational cost remains almost constant as M grows. This is because in two-stage FP, the scattering matrix $\Theta \in \mathbb{C}^{M \times M}$ — the only design variable associated with BD-

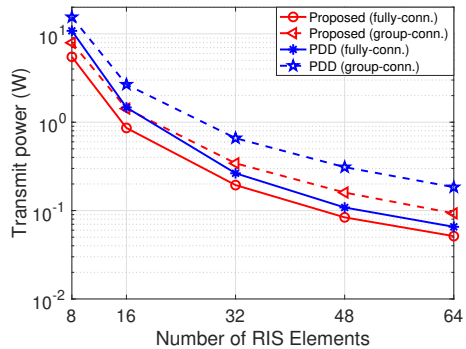


Fig. 5. Transmit power versus number of RIS elements ($N = K = 4, G_s = 4$).

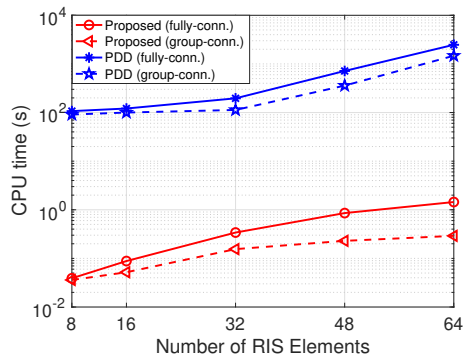


Fig. 6. CPU time versus number of RIS elements for transmit power minimization ($N = K = 4, G_s = 4$).

RIS — is first determined in a heuristic way and then held fixed while solving the sum-rate maximization problem. Though simple and efficient, such a heuristic approach lacks theoretical justification and leads to performance loss.

In Figs. 5 and 6, we examine the transmit power minimization problem, comparing the performance and CPU time of the proposed pp-ADMM algorithm with the PDD algorithm in [31]. The results show that the proposed pp-ADMM algorithm is able to achieve lower transmit power than PDD with substantially reduced CPU time, demonstrating both its effectiveness and the efficiency. We remark that for both sum-rate maximization and transmit power minimization problems, the superiority in computational efficiency of pp-ADMM over PDD is more prominent as N and K grow. Detailed simulation results are omitted here due to space limitations.

In Figs. 7 and 8, we compare the performance of the four BD-RIS architectures introduced in Section II-B, where Fig. 7 presents the result for sum-rate maximization and Fig. 8 shows the result for transmit power minimization. As expected, the fully-connected and single-connected RIS demonstrate the best and worst performance, respectively, due to the highest and lowest design flexibility they offer. The tree-connected RIS, though proven optimal for single-user MISO systems [8], suffers from a performance degradation compared to fully-connected RIS in multi-user MISO systems and is thus no longer optimal. Nevertheless, we can observe that the tree-connected RIS achieves performance comparable to the group-connected RIS with group size $G_s = 4$, while requiring fewer impedances (the impedances are $2N - 1$ and $2.5N$, respec-

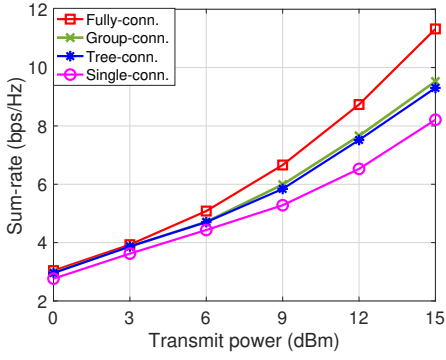


Fig. 7. Sum-rate versus transmit power for different BD-RIS architectures ($N = K = 4, M = 32, G_s = 4$).

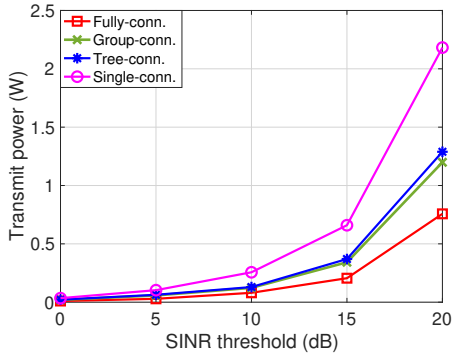


Fig. 8. Transmit power versus SINR threshold for different BD-RIS architectures ($N = K = 4, M = 32, G_s = 4$).

tively, for tree-connected RIS and group-connected RIS with $G_s = 4$). This suggests that the tree-connected architecture may still be preferable to the group-connected ones in multi-user systems, possibly due to its “more connected” circuit topology.

Based on the above observation, a natural yet important question arises: what is the optimal BD-RIS architecture in multi-user scenarios? We leave this as an intriguing direction for future work.

VII. CONCLUSION

This paper studied the optimization of BD-RIS, focusing mainly on sum-rate maximization and transmit power minimization for MU-MISO systems. For each problem, we custom-developed a partially proximal ADMM algorithm. The proposed algorithms offer several advantages. First, they are architecture-independent and thus applicable to any BD-RIS architecture. Second, they are computationally efficient, with each subproblem in the ADMM framework either admitting a closed-form solution or being solvable with low complexity. Finally, they exhibit desirable theoretical convergence properties under mild assumptions. The proposed framework can also be extended to encompass other utility functions and MU-MIMO systems. Extensive simulation results demonstrate that our approaches achieve better trade-off between performance and CPU time compared to existing state-of-the-art methods. Another interesting insight drawn from our simulations is that the tree-connected RIS — known to be optimal in single-user MISO systems — is no longer optimal in multi-user systems.

As an important direction of future work, we aim to identify the optimal BD-RIS architectures for multi-user systems.

APPENDIX A PROOF OF (29)

In this appendix, we prove that (29) is the optimal solution to problem (28).

We first examine the KKT condition of problem (28). Let η and ν be the Lagrange multipliers associated with the first and second constraints of problem (28), respectively. The KKT condition is given by

$$\begin{cases} (1 - \eta)r_{k,k} = a_{k,k} + \nu/2, & \text{if } j = k; \\ (1 + \Gamma_k \eta)r_{k,j} = a_{k,j}, & \text{if } j \neq k, \end{cases} \quad (37a)$$

$$\eta \left(r_{k,k}^2 - \Gamma_k \left(\sum_{j \neq k} r_{k,j}^2 + \sigma^2 \right) \right) = 0, \quad (37b)$$

$$r_{k,k}^2 \geq \Gamma_k \left(\sum_{j \neq k} r_{k,j}^2 + \sigma^2 \right), \quad \eta \geq 0, \quad (37c)$$

$$\nu r_{k,k} = 0, \quad \nu \geq 0, \quad r_{k,k} \geq 0. \quad (37d)$$

It follows from (37c) and (37d) that $r_{k,k} > 0$ and $\nu = 0$. This, combined with the expression of $r_{k,k}$ in (37a), implies that $\eta \in [0, 1)$ when $a_{k,k} > 0$, $\eta = 1$ when $a_{k,k} = 0$, and $\eta \in (1, \infty)$ otherwise. Clearly, when $a_{k,k} = 0$, the solution given by (29) is the unique KKT point satisfying (37). Next, we investigate the case that $a_{k,k} \neq 0$. Consider the following function:

$$\begin{aligned} h(\eta) &= r_{k,k}^2 - \Gamma_k \left(\sum_{j \neq k} r_{k,j}^2 + \sigma^2 \right) \\ &= \frac{a_{k,k}^2}{(1 - \eta)^2} - \frac{\Gamma_k \sum_{j \neq k} a_{k,j}^2}{(1 + \Gamma_k \eta)^2} - \Gamma_k \sigma^2, \end{aligned}$$

where the second equation is due to (37a) and the fact that $\nu = 0$. Then (37b) and (37c) can be expressed as

$$\eta h(\eta) = 0, \quad \eta \geq 0, \quad h(\eta) \geq 0.$$

It is straightforward to check that

$$\begin{aligned} h(0) &= a_{k,k}^2 - \Gamma_k \sum_{j \neq k} a_{k,j}^2 - \Gamma_k \sigma^2, \\ \lim_{\eta \rightarrow 1} h(\eta) &= \infty, \quad \lim_{\eta \rightarrow \infty} h(\eta) = -\Gamma_k \sigma^2 < 0. \end{aligned} \quad (38)$$

Therefore, η given in (30) is well-defined (i.e., η_1^* and η_2^* exist) and the solution given by (29) satisfies the KKT condition in (37). In addition, according to

$$h'(\eta) = 2\Gamma_k^2 \sum_{j \neq k} a_{k,j}^2 (1 + \Gamma_k \eta)^{-3} + 2a_{k,k}^2 (1 - \eta)^{-3},$$

$h(\eta)$ is increasing in $(0, 1)$. Since there is at most one solution to $h'(\eta) = 0$ in $(1, \infty)$, $h(\eta)$ is either decreasing or first decreasing and then increasing in $(1, \infty)$. This, combined with (38), implies the uniqueness of η_1^* and η_2^* . Therefore, the solution given by (29) is the unique KKT point of (28), which is thus the optimal solution to (28).

APPENDIX B
PROOF OF THEOREM 1

Our proof follows a similar idea to the classical proof in [45], [46], which contains three main steps. First, we show that the difference between the Lagrangian multipliers in successive iterates can be bounded by that between the primal variables. With this result, the second step establishes a sufficient decrease condition for the augmented Lagrangian function. Finally, we investigate the limiting behavior of the sequence generated by the proposed pp-ADMM algorithm, based on the conclusions from the first two steps and the update rules in (11a) – (11f).

Next, we first present the results for the first and second steps as two auxiliary lemmas in Appendix B-A, and then conduct the final step to prove Theorem 1 in Appendix B-B.

A. Auxiliary Lemmas

Lemma 1. *Under the assumption in Theorem 1, there exists a constant C_0 independent of ρ such that*

$$\begin{aligned} \|\boldsymbol{\lambda}^{t+1} - \boldsymbol{\lambda}^t\|_2^2 &\leq C_0(\|\mathbf{y}^{t+1} - \mathbf{y}^t\|_2^2 + \|\boldsymbol{\gamma}^{t+1} - \boldsymbol{\gamma}^t\|_2^2 \\ &+ \|\mathbf{B}^{t+1} - \mathbf{B}^t\|_F^2 + \|\mathbf{W}^{t+1} - \mathbf{W}^t\|_F^2 + \|\mathbf{U}^{t+1} - \mathbf{U}^t\|_F^2). \end{aligned}$$

Proof. According to the update rule of variable \mathbf{U} in (11e), we have

$$\nabla_{\mathbf{U}} \mathcal{L}_\rho(\mathbf{y}^{t+1}, \boldsymbol{\gamma}^{t+1}, \mathbf{W}^{t+1}, \mathbf{B}^{t+1}, \mathbf{U}^{t+1}, \boldsymbol{\lambda}^t) = \mathbf{0},$$

which implies that

$$\begin{aligned} &\nabla_{\mathbf{U}} \tilde{R}(\mathbf{y}^{t+1}, \boldsymbol{\gamma}^{t+1}, \mathbf{W}^{t+1}, \mathbf{U}^{t+1}) \\ &- (\mathbf{I} + iZ_0\mathbf{B}^{t+1})(\boldsymbol{\lambda}^t + \rho((\mathbf{I} - iZ_0\mathbf{B}^{t+1})\mathbf{U}^{t+1} - (\mathbf{I} + iZ_0\mathbf{B}^{t+1})\mathbf{H})) \\ &= \nabla_{\mathbf{U}} \tilde{R}(\mathbf{y}^{t+1}, \boldsymbol{\gamma}^{t+1}, \mathbf{W}^{t+1}, \mathbf{U}^{t+1}) - (\mathbf{I} + iZ_0\mathbf{B}^{t+1})\boldsymbol{\lambda}^{t+1} = \mathbf{0}, \end{aligned}$$

where the first equality uses the update rule of the Lagrange multiplier $\boldsymbol{\lambda}$ in (11f). We claim that for any $t \geq 0$, the matrix $\mathbf{I} + iZ_0\mathbf{B}^t$ is invertible with

$$\|(\mathbf{I} + iZ_0\mathbf{B}^t)^{-1}\|_2 \leq 1. \quad (39)$$

This can be seen by expressing the matrix $\mathbf{I} + iZ_0\mathbf{B}^t$ as

$$\mathbf{I} + iZ_0\mathbf{B}^t = \mathbf{V}(iZ_0\mathbf{D} + \mathbf{I})\mathbf{V}^T,$$

where $\mathbf{B}^{t+1} = \mathbf{V}\mathbf{D}\mathbf{V}^T$ is the singular value decomposition of \mathbf{B}^t . Hence, $\boldsymbol{\lambda}^{t+1}$ can be expressed as

$$\boldsymbol{\lambda}^{t+1} = (\mathbf{I} + iZ_0\mathbf{B}^{t+1})^{-1} \nabla_{\mathbf{U}} \tilde{R}(\mathbf{y}^{t+1}, \boldsymbol{\gamma}^{t+1}, \mathbf{W}^{t+1}, \mathbf{U}^{t+1}). \quad (40)$$

Let $\nabla_{\mathbf{U}} \tilde{R}^t := \nabla_{\mathbf{U}} \tilde{R}(\mathbf{y}^t, \boldsymbol{\gamma}^t, \mathbf{W}^t, \mathbf{U}^t)$. It follows from (40) that

$$\begin{aligned} &\|\boldsymbol{\lambda}^{t+1} - \boldsymbol{\lambda}^t\|_F^2 \\ &\leq 2 \left\| (\mathbf{I} + iZ_0\mathbf{B}^{t+1})^{-1} \left(\nabla_{\mathbf{U}} \tilde{R}^{t+1} - \nabla_{\mathbf{U}} \tilde{R}^t \right) \right\|_F^2 \\ &\quad + 2 \left\| \left((\mathbf{I} + iZ_0\mathbf{B}^{t+1})^{-1} - (\mathbf{I} + iZ_0\mathbf{B}^t)^{-1} \right) \nabla_{\mathbf{U}} \tilde{R}^t \right\|_F^2 \\ &\leq 2 \left\| \nabla_{\mathbf{U}} \tilde{R}^{t+1} - \nabla_{\mathbf{U}} \tilde{R}^t \right\|_F^2 + 2Z_0^2 \|\nabla_{\mathbf{U}} \tilde{R}^t\|_2^2 \|\mathbf{B}^{t+1} - \mathbf{B}^t\|_F^2, \end{aligned} \quad (41)$$

where the last inequality uses (39), the fact that $\|\mathbf{X}\mathbf{Y}\|_F \leq \|\mathbf{X}\|_2 \|\mathbf{Y}\|_F$ for any given matrices \mathbf{X} and \mathbf{Y} , and

$$\begin{aligned} &(\mathbf{I} + iZ_0\mathbf{B}^{t+1})^{-1} - (\mathbf{I} + iZ_0\mathbf{B}^t)^{-1} \\ &= iZ_0(\mathbf{I} + iZ_0\mathbf{B}^{t+1})^{-1}(\mathbf{B}^t - \mathbf{B}^{t+1})(\mathbf{I} + iZ_0\mathbf{B}^t)^{-1}. \end{aligned}$$

Note that $\{\mathbf{W}^t\}_{t \geq 0}$ is bounded due to the total transmit power constraint. Under the assumption in Theorem 1, $\{\mathbf{U}^t\}_{t \geq 0}$ is bounded. Then it follows from (12) and (13) that $\{\mathbf{y}^t\}_{t \geq 0}$ and $\{\boldsymbol{\gamma}^t\}_{t \geq 0}$ are bounded. Since $\nabla_{\mathbf{U}} \tilde{R}^t$ is continuously differentiable, it is bounded and Lipschitz continuous on any compact set, i.e., there exists constants $C_{0,1}$ and $C_{0,2}$ such that $\|\nabla_{\mathbf{U}} \tilde{R}^t\|_2^2 \leq C_{0,1}$ and

$$\begin{aligned} \left\| \nabla_{\mathbf{U}} \tilde{R}^{t+1} - \nabla_{\mathbf{U}} \tilde{R}^t \right\|_F^2 &\leq C_{0,2}(\|\mathbf{y}^{t+1} - \mathbf{y}^t\|_2^2 + \|\boldsymbol{\gamma}^{t+1} - \boldsymbol{\gamma}^t\|_2^2 \\ &\quad + \|\mathbf{W}^{t+1} - \mathbf{W}^t\|_F^2 + \|\mathbf{U}^{t+1} - \mathbf{U}^t\|_F^2). \end{aligned}$$

Combining the above discussions with (41), we can conclude that Lemma 1 holds with $C_0 = 2 \max\{Z_0^2 C_{0,1}, C_{0,2}\}$. \square

Lemma 2. *Let $\mathcal{L}_\rho^t := \mathcal{L}_\rho(\mathbf{y}^t, \boldsymbol{\gamma}^t, \mathbf{W}^t, \mathbf{B}^t, \mathbf{U}^t, \boldsymbol{\lambda}^t)$ denote the value of the augmented Lagrangian function in (10) at the t -th iteration. Then the following inequality holds:*

$$\begin{aligned} &\mathcal{L}_\rho^{t+1} - \mathcal{L}_\rho^t \\ &\geq \left(\frac{\sigma^2}{2} - \frac{C_0}{\rho} \right) \|\mathbf{y}^{t+1} - \mathbf{y}^t\|_2^2 + \left(\frac{1}{2(1+C_\gamma)^2} - \frac{C_0}{\rho} \right) \|\boldsymbol{\gamma}^{t+1} - \boldsymbol{\gamma}^t\|_2^2 \\ &\quad + \left(\frac{\tau}{2} - \frac{C_0}{\rho} \right) \|\mathbf{W}^{t+1} - \mathbf{W}^t\|_F^2 + \left(\frac{\xi}{2} - \frac{C_0}{\rho} \right) \|\mathbf{B}^{t+1} - \mathbf{B}^t\|_F^2 \\ &\quad + \left(\frac{\rho}{2} - \frac{C_0}{\rho} \right) \|\mathbf{U}^{t+1} - \mathbf{U}^t\|_F^2, \end{aligned} \quad (42)$$

where C_γ is an upper bound⁶ on $\|\boldsymbol{\gamma}^t\|_\infty$, C_0 is given in Lemma 1, τ and ρ are algorithm parameters; see (11).

Proof. The proof is based on the fact that given a strongly concave function $f(\mathbf{x})$ with modulus μ and a convex set \mathcal{C} , the following inequality holds for $\mathbf{x}^* \in \arg \max_{\mathbf{x} \in \mathcal{C}} f(\mathbf{x})$:

$$f(\mathbf{x}^*) - f(\mathbf{x}) \geq \frac{\mu}{2} \|\mathbf{x} - \mathbf{x}^*\|_2^2, \quad \forall \mathbf{x} \in \mathcal{C}.$$

When the variable is a matrix, the ℓ_2 norm on the r.h.s. should be replaced by the Frobenius norm. Applying this result to the \mathbf{y} -, $\boldsymbol{\gamma}$ -, \mathbf{W} -, \mathbf{B} -, and \mathbf{U} -subproblems in (11a)–(11e), whose objective functions are strongly concave with modulus σ^2 , $(1+C_\gamma)^{-2}$, τ , ξ , and ρ , respectively, we get

$$\begin{aligned} &\mathcal{L}_\rho(\mathbf{y}^{t+1}, \boldsymbol{\gamma}^{t+1}, \mathbf{W}^{t+1}, \mathbf{B}^{t+1}, \mathbf{U}^{t+1}, \boldsymbol{\lambda}^t) \\ &- \mathcal{L}_\rho(\mathbf{y}^t, \boldsymbol{\gamma}^t, \mathbf{W}^t, \mathbf{B}^t, \mathbf{U}^t, \boldsymbol{\lambda}^t) \\ &\geq \frac{\sigma^2}{2} \|\mathbf{y}^{t+1} - \mathbf{y}^t\|_2^2 + \frac{1}{2(1+C_\gamma)^2} \|\boldsymbol{\gamma}^{t+1} - \boldsymbol{\gamma}^t\|_2^2 \\ &\quad + \frac{\tau}{2} \|\mathbf{W}^{t+1} - \mathbf{W}^t\|_F^2 + \frac{\xi}{2} \|\mathbf{B}^{t+1} - \mathbf{B}^t\|_F^2 + \frac{\rho}{2} \|\mathbf{U}^{t+1} - \mathbf{U}^t\|_F^2. \end{aligned} \quad (43)$$

In addition, using the formula of the augmented Lagrangian function in (10), we have

$$\begin{aligned} &\mathcal{L}_\rho(\mathbf{y}^{t+1}, \boldsymbol{\gamma}^{t+1}, \mathbf{W}^{t+1}, \mathbf{B}^{t+1}, \mathbf{U}^{t+1}, \boldsymbol{\lambda}^{t+1}) \\ &- \mathcal{L}_\rho(\mathbf{y}^{t+1}, \boldsymbol{\gamma}^{t+1}, \mathbf{W}^{t+1}, \mathbf{B}^{t+1}, \mathbf{U}^{t+1}, \boldsymbol{\lambda}^t) \\ &= -\langle \boldsymbol{\lambda}^{t+1} - \boldsymbol{\lambda}^t, (\mathbf{I} - iZ_0\mathbf{B}^{t+1})\mathbf{U}^{t+1} - (\mathbf{I} + iZ_0\mathbf{B}^{t+1})\mathbf{H} \rangle \\ &= -\frac{1}{\rho} \|\boldsymbol{\lambda}^{t+1} - \boldsymbol{\lambda}^t\|_F^2 \end{aligned} \quad (44)$$

where the second equality uses the update rule of $\boldsymbol{\lambda}$ in (11f). Combining (43) and (44) and applying Lemma 1 to (44) gives the desired result in Lemma 2. \square

⁶ C_γ exists due to the boundedness of $\{\mathbf{W}^t\}$, $\{\mathbf{U}^t\}$; see discussions in the proof of Lemma 1.

B. Proof of Theorem 1

Now we are ready to prove Theorem 1. Given $T > 0$, summing over (42) from $t = 0$ to $t = T$ gives

$$\begin{aligned} & \mathcal{L}_\rho^{T+1} - \mathcal{L}_\rho^0 \\ & \geq \left(\frac{\sigma^2}{2} - \frac{C_0}{\rho} \right) \sum_{t=0}^T \|\mathbf{y}^{t+1} - \mathbf{y}^t\|_2^2 + \left(\frac{\xi}{2} - \frac{C_0}{\rho} \right) \sum_{t=1}^T \|\mathbf{B}^{t+1} - \mathbf{B}^t\|_F^2 \\ & \quad + \left(\frac{1}{2(1+C_\gamma)^2} - \frac{C_0}{\rho} \right) \sum_{t=0}^T \|\gamma^{t+1} - \gamma^t\|_2^2 \\ & \quad + \left(\frac{\tau}{2} - \frac{C_0}{\rho} \right) \sum_{t=0}^T \|\mathbf{W}^{t+1} - \mathbf{W}^t\|_F^2 + \left(\frac{\rho}{2} - \frac{C_0}{\rho} \right) \sum_{t=0}^T \|\mathbf{U}^{t+1} - \mathbf{U}^t\|_F^2. \end{aligned} \quad (45)$$

Let

$$\rho_0 = \max \left\{ \frac{2C_0}{\sigma^2}, \frac{2C_0}{\tau}, \frac{2C_0}{\xi}, \sqrt{2C_0}, 2(1+C_\gamma)^2 C_0 \right\}.$$

It is straightforward to check that if $\rho > \rho_0$, the factor in front of each term in (45) is positive. In addition, $\{\mathcal{L}_\rho^t\}_{t \geq 0}$ is bounded from above under boundedness assumption on $\{\mathbf{U}^t\}_{t \geq 0}$ and $\{\boldsymbol{\lambda}^t\}_{t \geq 0}$. Therefore, letting $T \rightarrow \infty$ in (45) yields

$$\begin{aligned} \|\mathbf{y}^{t+1} - \mathbf{y}^t\|_2 & \rightarrow 0, \quad \|\gamma^{t+1} - \gamma^t\|_2 \rightarrow 0, \quad \|\mathbf{W}^{t+1} - \mathbf{W}^t\|_F \rightarrow 0, \\ \|\mathbf{B}^{t+1} - \mathbf{B}^t\|_F & \rightarrow 0, \quad \|\mathbf{U}^{t+1} - \mathbf{U}^t\|_F \rightarrow 0. \end{aligned}$$

It further follows from Lemma 1 that $\|\boldsymbol{\lambda}^{t+1} - \boldsymbol{\lambda}^t\|_F \rightarrow 0$. According to the update rule of the proposed pp-ADMM algorithm in (11), we have

$$\nabla_{\mathbf{y}} \tilde{R}(\mathbf{y}^{t+1}, \gamma^t, \mathbf{W}^t, \mathbf{U}^t) = \mathbf{0}, \quad (46a)$$

$$\nabla_{\gamma} \tilde{R}(\mathbf{y}^{t+1}, \gamma^{t+1}, \mathbf{W}^t, \mathbf{U}^t) = \mathbf{0}, \quad (46b)$$

$$\begin{aligned} & \langle \nabla_{\mathbf{W}} \tilde{R}(\mathbf{y}^{t+1}, \gamma^{t+1}, \mathbf{W}^{t+1}, \mathbf{U}^t) \\ & \quad - \tau(\mathbf{W}^{t+1} - \mathbf{W}^t), \mathbf{W} - \mathbf{W}^{t+1} \rangle \leq 0, \quad \forall \mathbf{W}: \|\mathbf{W}\|_F^2 \leq P_T, \end{aligned} \quad (46c)$$

$$\begin{aligned} & \langle (\boldsymbol{\lambda}^{t+1} - \rho(\mathbf{I} - iZ_0\mathbf{B}^{t+1})(\mathbf{U}^{t+1} - \mathbf{U}^t)) (iZ_0\mathbf{U}^t + iZ_0\mathbf{H})^\dagger \\ & \quad + \xi(\mathbf{B}^{t+1} - \mathbf{B}^t), \mathbf{B} - \mathbf{B}^{t+1} \rangle \geq 0, \quad \forall \mathbf{B}: \mathbf{B} = \mathbf{B}^T, \mathbf{B} \in \mathcal{B}, \end{aligned} \quad (46d)$$

$$\nabla_{\mathbf{U}} \tilde{R}(\mathbf{y}^{t+1}, \gamma^{t+1}, \mathbf{W}^{t+1}, \mathbf{U}^{t+1}) - (\mathbf{I} + iZ_0\mathbf{B}^{t+1})\boldsymbol{\lambda}^{t+1} = \mathbf{0}, \quad (46e)$$

$$\boldsymbol{\lambda}^{t+1} = \boldsymbol{\lambda}^t + \rho((\mathbf{I} - iZ_0\mathbf{B}^{t+1})\mathbf{U}^{t+1} - (\mathbf{I} + iZ_0\mathbf{B}^{t+1})\mathbf{H}), \quad (46f)$$

Let $(\mathbf{y}^*, \gamma^*, \mathbf{W}^*, \mathbf{B}^*, \mathbf{U}^*, \boldsymbol{\lambda}^*)$ be a limit point of $(\mathbf{y}^t, \gamma^t, \mathbf{W}^t, \mathbf{B}^t, \mathbf{U}^t, \boldsymbol{\lambda}^t)$ with

$$\lim_{j \rightarrow \infty} (\mathbf{y}^{t_j}, \gamma^{t_j}, \mathbf{W}^{t_j}, \mathbf{B}^{t_j}, \mathbf{U}^{t_j}, \boldsymbol{\lambda}^{t_j}) = (\mathbf{y}^*, \gamma^*, \mathbf{W}^*, \mathbf{B}^*, \mathbf{U}^*, \boldsymbol{\lambda}^*).$$

Then substituting $t = t_j$ in (50) and letting $j \rightarrow \infty$ gives

$$\nabla_{\mathbf{y}} \tilde{R}(\mathbf{y}^*, \gamma^*, \mathbf{W}^*, \mathbf{U}^*) = \mathbf{0}, \quad (47a)$$

$$\nabla_{\gamma} \tilde{R}(\mathbf{y}^*, \gamma^*, \mathbf{W}^*, \mathbf{U}^*) = \mathbf{0}, \quad (47b)$$

$$\begin{aligned} & \langle \nabla_{\mathbf{W}} \tilde{R}(\mathbf{y}^*, \gamma^*, \mathbf{W}^*, \mathbf{U}^*), \mathbf{W} - \mathbf{W}^* \rangle \leq 0, \\ & \quad \forall \mathbf{W}: \|\mathbf{W}\|_F^2 \leq P_T, \end{aligned} \quad (47c)$$

$$\begin{aligned} & \langle \boldsymbol{\lambda}^* (iZ_0\mathbf{U}^* + iZ_0\mathbf{H})^\dagger, \mathbf{B} - \mathbf{B}^* \rangle \geq 0, \quad \forall \mathbf{B}: \mathbf{B} = \mathbf{B}^T, \mathbf{B} \in \mathcal{B}, \\ & \quad (47d) \end{aligned}$$

$$\nabla_{\mathbf{U}} \tilde{R}(\mathbf{y}^*, \gamma^*, \mathbf{W}^*, \mathbf{U}^*) - (\mathbf{I} + iZ_0\mathbf{B}^*)\boldsymbol{\lambda}^* = \mathbf{0}, \quad (47e)$$

$$(\mathbf{I} - iZ_0\mathbf{B}^*)\mathbf{U}^* - (\mathbf{I} + iZ_0\mathbf{B}^*)\mathbf{H} = \mathbf{0}, \quad (47f)$$

i.e., $(\mathbf{y}^*, \gamma^*, \mathbf{W}^*, \mathbf{B}^*, \mathbf{U}^*)$ is a stationary point of problem (9), with $\boldsymbol{\lambda}^*$ being the Lagrangian multiplier associated with the bilinear constraint (7b).

APPENDIX C PROOF OF THEOREM 2

The proof of Theorem 2 follows the same procedure as that of Theorem 1. The main difference is that there are two bilinear constraints in problem (23), which couple the three variables $(\mathbf{W}, \mathbf{U}, \mathbf{B})$ and complicate the relationship between the primal and dual variables. As a result, the proof is slightly more involved.

Following the same structure as the proof of Theorem 1, we begin by presenting two auxiliary lemmas, which, respectively, bound the difference between successive iterations of dual variables with that of primal variables, and demonstrate the sufficient decrease property of a properly defined potential function. Then, we give the proof of Theorem 2.

Lemma 3. *Under the assumptions in Theorem 2, there exists constants $C_0 > 0$ and $C_1 > 0$ such that*

$$\begin{aligned} \|\boldsymbol{\lambda}^{t+1} - \boldsymbol{\lambda}^t\|_F^2 & \leq C_0 (\|\mathbf{W}^{t+1} - \mathbf{W}^t\|_F^2 \\ & \quad + \|\mathbf{B}^{t+1} - \mathbf{B}^t\|_F^2 + \|\boldsymbol{\mu}^{t+1} - \boldsymbol{\mu}^t\|_F^2) \end{aligned}$$

and

$$\begin{aligned} \|\boldsymbol{\mu}^{t+1} - \boldsymbol{\mu}^t\|_F^2 & \leq C_1 (\|\mathbf{W}^{t+1} - \mathbf{W}^t\|_F^2 + \|\mathbf{U}^{t+1} - \mathbf{U}^t\|_F^2) \\ & \quad + C_1 \rho_\mu^2 (\|\mathbf{U}^{t+1} - \mathbf{U}^t\|_F^2 + \|\mathbf{U}^t - \mathbf{U}^{t-1}\|_F^2). \end{aligned}$$

Proof. First, by combining the optimality conditions of (26b) and (26d) with (26e) and (26f), we get

$$\boldsymbol{\lambda}^{t+1} = (\mathbf{I} + iZ_0\mathbf{B}^{t+1})^{-1} \mathbf{G} \mathbf{W}^{t+1} (\boldsymbol{\mu}^{t+1})^\dagger$$

and

$$\begin{aligned} \boldsymbol{\mu}^{t+1} & = 2((\mathbf{U}^t)^\dagger \mathbf{G} \mathbf{G}^\dagger \mathbf{U}^t)^{-1} (\mathbf{U}^t)^\dagger \mathbf{G} \mathbf{W}^{t+1} \\ & \quad - \rho_\mu (\mathbf{U}^{t+1} - \mathbf{U}^t)^\dagger \mathbf{G} \mathbf{W}^{t+1}. \end{aligned}$$

Then, applying a similar argument as in Lemma 1 gives the first assertion of Lemma 3. For $\boldsymbol{\mu}$, using the expression above, we have

$$\begin{aligned} \boldsymbol{\mu}^{t+1} - \boldsymbol{\mu}^t & = 2((\mathbf{U}^t)^\dagger \mathbf{G} \mathbf{G}^\dagger \mathbf{U}^t)^{-1} (\mathbf{U}^t)^\dagger \mathbf{G} \mathbf{W}^{t+1} \\ & \quad - 2((\mathbf{U}^{t-1})^\dagger \mathbf{G} \mathbf{G}^\dagger \mathbf{U}^{t-1})^{-1} (\mathbf{U}^{t-1})^\dagger \mathbf{G} \mathbf{W}^t \\ & \quad - \rho_\mu (\mathbf{U}^{t+1} - \mathbf{U}^t)^\dagger \mathbf{G} \mathbf{W}^{t+1} \\ & \quad + \rho_\mu (\mathbf{U}^t - \mathbf{U}^{t-1})^\dagger \mathbf{G} \mathbf{W}^t. \end{aligned} \quad (48)$$

Note that for two full-rank matrices \mathbf{X}_1 and \mathbf{X}_2 , the following inequality holds:

$$\begin{aligned} & \|(\mathbf{X}_1 \mathbf{X}_1^\dagger)^{-1} \mathbf{X}_1 - (\mathbf{X}_2 \mathbf{X}_2^\dagger)^{-1} \mathbf{X}_2\|_F \\ & \leq \|(\mathbf{X}_1 \mathbf{X}_1^\dagger)^{-1} - (\mathbf{X}_2 \mathbf{X}_2^\dagger)^{-1}\|_F \|\mathbf{X}_1\|_2 \\ & \quad + \|(\mathbf{X}_2 \mathbf{X}_2^\dagger)^{-1}\|_2 \|\mathbf{X}_1 - \mathbf{X}_2\|_F \\ & \leq \|(\mathbf{X}_1 \mathbf{X}_1^\dagger)^{-1}\|_2 \|(\mathbf{X}_2 \mathbf{X}_2^\dagger)^{-1}\|_2 \|\mathbf{X}_1\|_2 \|\mathbf{X}_1 \mathbf{X}_1^\dagger - \mathbf{X}_2 \mathbf{X}_2^\dagger\|_F \\ & \quad + \|(\mathbf{X}_2 \mathbf{X}_2^\dagger)^{-1}\|_2 \|\mathbf{X}_1 - \mathbf{X}_2\|_F \\ & \leq \left(\|(\mathbf{X}_1 \mathbf{X}_1^\dagger)^{-1}\|_2 \|(\mathbf{X}_2 \mathbf{X}_2^\dagger)^{-1}\|_2 \|\mathbf{X}_1\|_2 (\|\mathbf{X}_1\|_2 + \|\mathbf{X}_2\|_2) \right. \\ & \quad \left. + \|(\mathbf{X}_2 \mathbf{X}_2^\dagger)^{-1}\|_2 \right) \|\mathbf{X}_1 - \mathbf{X}_2\|_F. \end{aligned}$$

Applying the above inequality with $\mathbf{X}_1 = (\mathbf{U}^{t-1})^\dagger \mathbf{G}$ and $\mathbf{X}_2 = (\mathbf{U}^t)^\dagger \mathbf{G}$, and utilizing (48), we can conclude that under the assumptions in Theorem 2, there exists $C_1 > 0$ such the second assertion in Lemma 3 holds. \square

Lemma 4. *Define*

$$\tilde{\mathcal{L}}_\rho^t := \mathcal{L}_\rho^t + \left(\frac{C_0 C_1 \rho_\mu^2}{\rho_\lambda} + C_1 \rho_\mu \right) \|\mathbf{U}^t - \mathbf{U}^{t-1}\|_F^2,$$

where $\mathcal{L}_\rho^t := \mathcal{L}_\rho(\mathbf{Y}^t, \mathbf{W}^t, \mathbf{B}^t, \mathbf{U}^t, \boldsymbol{\lambda}^t, \boldsymbol{\mu}^t)$. It holds that

$$\begin{aligned} & \tilde{\mathcal{L}}_\rho^{t+1} - \tilde{\mathcal{L}}_\rho^t \\ & \leq -\frac{\rho_\mu}{2} \|\mathbf{Y}^{t+1} - \mathbf{Y}^t\|_F^2 - \left(\frac{\xi}{2} - \frac{C_0}{\rho_\lambda} \right) \|\mathbf{B}^{t+1} - \mathbf{B}^t\|_F^2 \\ & \quad - \left(1 - \frac{C_0 + C_0 C_1}{\rho_\lambda} - \frac{C_1}{\rho_\mu} \right) \|\mathbf{W}^{t+1} - \mathbf{W}^t\|_F^2 \\ & \quad - \left(\frac{\rho_\lambda}{2} - \frac{C_0 C_1}{\rho_\lambda} - \frac{C_1}{\rho_\mu} - \frac{2C_0 C_1 \rho_\mu^2}{\rho_\lambda} - 2C_1 \rho_\mu \right) \|\mathbf{U}^{t+1} - \mathbf{U}^t\|_F^2. \end{aligned} \quad (49)$$

Proof. We first note that the objective functions of the \mathbf{Y} -, \mathbf{W} -, \mathbf{B} -, and \mathbf{U} -subproblems in (26a)–(26d) are all strongly convex, with modulus ρ_μ , 2, ξ , and ρ_λ , respectively. Hence, similar to the proof of Lemma 2, we have

$$\begin{aligned} & \mathcal{L}_\rho^{t+1} - \mathcal{L}_\rho^t \\ & \leq -\frac{\rho_\mu}{2} \|\mathbf{Y}^{t+1} - \mathbf{Y}^t\|_F^2 - \frac{\xi}{2} \|\mathbf{B}^{t+1} - \mathbf{B}^t\|_F^2 - \|\mathbf{W}^{t+1} - \mathbf{W}^t\|_F^2 \\ & \quad - \frac{\rho_\lambda}{2} \|\mathbf{U}^{t+1} - \mathbf{U}^t\|_F^2 + \frac{\rho_\lambda}{\rho_\lambda} \|\boldsymbol{\lambda}^{t+1} - \boldsymbol{\lambda}^t\|_F^2 + \frac{\|\boldsymbol{\mu}^{t+1} - \boldsymbol{\mu}^t\|_F^2}{\rho_\mu} \\ & \leq -\frac{\rho_\mu}{2} \|\mathbf{Y}^{t+1} - \mathbf{Y}^t\|_F^2 - \left(\frac{\xi}{2} - \frac{C_0}{\rho_\lambda} \right) \|\mathbf{B}^{t+1} - \mathbf{B}^t\|_F^2 \\ & \quad - \left(1 - \frac{C_0 + C_0 C_1}{\rho_\lambda} - \frac{C_1}{\rho_\mu} \right) \|\mathbf{W}^{t+1} - \mathbf{W}^t\|_F^2 \\ & \quad - \left(\frac{\rho_\lambda}{2} - \frac{C_0 C_1}{\rho_\lambda} - \frac{C_1}{\rho_\mu} - \frac{C_0 C_1 \rho_\mu^2}{\rho_\lambda} - C_1 \rho_\mu \right) \|\mathbf{U}^{t+1} - \mathbf{U}^t\|_F^2 \\ & \quad + \left(\frac{C_0 C_1 \rho_\mu^2}{\rho_\lambda} + C_1 \rho_\mu \right) \|\mathbf{U}^t - \mathbf{U}^{t-1}\|_F^2, \end{aligned}$$

where the first inequality follows from the strong convexity of each subproblem and the update rules of the Lagrange multipliers, and the second inequality is obtained by applying Lemma 3. Then Lemma 4 follows immediately by adding $(C_0 C_1 \rho_\mu^2 / \rho_\lambda + C_1 \rho_\mu)(\|\mathbf{U}^{t+1} - \mathbf{U}^t\|_F^2 - \|\mathbf{U}^t - \mathbf{U}^{t-1}\|_F^2)$ to both sides of the above expression. \square

Proof of Theorem 2: It is straightforward to see that we can choose sufficiently large c_0 and ρ_0 in Theorem 2 such that each term in the r.h.s. of Lemma 4 is positive. Then, by summing over (49) from $t = 0$ to $t = T$ and noting the lower boundedness of $\tilde{\mathcal{L}}_\rho^t$, we can show that

$$\begin{aligned} \|\mathbf{Y}^{t+1} - \mathbf{Y}^t\|_F & \rightarrow 0, \quad \|\mathbf{W}^{t+1} - \mathbf{W}^t\|_F \rightarrow 0, \\ \|\mathbf{B}^{t+1} - \mathbf{B}^t\|_F & \rightarrow 0, \quad \|\mathbf{U}^{t+1} - \mathbf{U}^t\|_F \rightarrow 0. \end{aligned}$$

Following similar steps as in Appendix B-B, we can get the desired result.

REFERENCES

- [1] Q. Wu and R. Zhang, "Intelligent reflecting surface enhanced wireless network via joint active and passive beamforming," *IEEE Trans. Wireless Commun.*, vol. 18, no. 11, pp. 5394–5409, Nov. 2019.
- [2] H. Guo, Y.-C. Liang, J. Chen, and E. G. Larsson, "Weighted sum-rate maximization for reconfigurable intelligent surface aided wireless networks," *IEEE Trans. Wireless Commun.*, vol. 19, no. 5, pp. 3064–3076, May 2020.
- [3] Q. Wu, S. Zhang, B. Zheng, C. You, and R. Zhang, "Intelligent reflecting surface-aided wireless communications: A tutorial," *IEEE Transactions Commun.*, vol. 69, no. 5, pp. 3313–3351, May 2021.
- [4] Y. Liu, X. Liu, X. Mu, T. Hou, J. Xu, M. Di Renzo, and N. Al-Dhahir, "Reconfigurable intelligent surfaces: Principles and opportunities," *IEEE Commun. Surveys Tuts.*, vol. 23, no. 3, pp. 1546–1577, 3rd Quart. 2021.
- [5] S. Shen, B. Clerckx, and R. Murch, "Modeling and architecture design of reconfigurable intelligent surfaces using scattering parameter network analysis," *IEEE Trans. Wireless Commun.*, vol. 21, no. 2, pp. 1229–1243, Feb. 2022.
- [6] H. Li, S. Shen, M. Nerini, and B. Clerckx, "Reconfigurable intelligent surfaces 2.0: Beyond diagonal phase shift matrices," *IEEE Commun. Mag.*, vol. 62, no. 3, pp. 102–108, Mar. 2024.
- [7] H. Li, S. Shen, and B. Clerckx, "Beyond diagonal reconfigurable intelligent surfaces: From transmitting and reflecting modes to single-, group-, and fully-connected architectures," *IEEE Trans. Wireless Commun.*, vol. 22, no. 4, pp. 2311–2324, Apr. 2023.
- [8] M. Nerini, S. Shen, H. Li, and B. Clerckx, "Beyond diagonal reconfigurable intelligent surfaces utilizing graph theory: Modeling, architecture design, and optimization," *IEEE Trans. Wireless Commun.*, vol. 23, no. 8, pp. 9972–9985, Aug. 2024.
- [9] M. Nerini and B. Clerckx, "Pareto frontier for the performance-complexity trade-off in beyond diagonal reconfigurable intelligent surfaces," *IEEE Commun. Lett.*, vol. 27, no. 10, pp. 2842–2846, Oct. 2023.
- [10] H. Li, S. Shen, and B. Clerckx, "Beyond diagonal reconfigurable intelligent surfaces: A multi-sector mode enabling highly directional full-space wireless coverage," *IEEE J. Sel. Areas Commun.*, vol. 41, no. 8, pp. 2446–2460, Aug. 2023.
- [11] M. Nerini, S. Shen, and B. Clerckx, "Discrete-value group and fully connected architectures for beyond diagonal reconfigurable intelligent surfaces," *IEEE Trans. Vehicular Tech.*, vol. 72, no. 12, pp. 16354–16368, Dec. 2023.
- [12] H. Li, S. Shen, M. Nerini, M. Di Renzo, and B. Clerckx, "Beyond diagonal reconfigurable intelligent surfaces with mutual coupling: Modeling and optimization," *IEEE Commun. Lett.*, vol. 28, no. 4, pp. 937–941, Apr. 2024.
- [13] M. Nerini, H. Li, and B. Clerckx, "Global optimal closed-form solutions for intelligent surfaces with mutual coupling: Is mutual coupling detrimental or beneficial?" 2024. [Online]. Available: <https://arxiv.org/abs/2411.04949>
- [14] H. Wang, Z. Han, and A. L. Swindlehurst, "Channel reciprocity attacks using intelligent surfaces with non-diagonal phase shifts," *IEEE Open J. Commun. Soc.*, vol. 5, pp. 1469–1485, 2024.
- [15] H. Li, M. Nerini, S. Shen, and B. Clerckx, "Beyond diagonal reconfigurable intelligent surfaces in wideband OFDM communications: Circuit-based modeling and optimization," 2024. [Online]. Available: <https://arxiv.org/abs/2405.07297>
- [16] M. Soleymani, I. Santamaria, A. Sezgin, and E. Jorswieck, "Maximizing spectral and energy efficiency in multi-user MIMO OFDM systems with RIS and hardware impairment," 2024. [Online]. Available: <https://arxiv.org/abs/2401.11921>
- [17] Ö. T. Demir and E. Björnson, "Wideband channel capacity maximization with beyond diagonal RIS reflection matrices," 2024. [Online]. Available: <https://arxiv.org/abs/2404.00982>
- [18] H. Li and B. Clerckx, "Non-reciprocal beyond diagonal RIS: Multipoint network models and performance benefits in full-duplex systems," 2024. [Online]. Available: <https://arxiv.org/abs/2411.04370>
- [19] B. Wang, H. Li, S. Shen, Z. Cheng, and B. Clerckx, "A dual-function radar-communication system empowered by beyond diagonal reconfigurable intelligent surface," *IEEE Trans. Commun. (early access)*, 2024.
- [20] A. Mahmood, T. X. Vu, W. U. Khan, S. Chatzinotas, and B. Ottersten, "Joint computation and communication resource optimization for beyond diagonal UAV-IRS empowered MEC networks," 2024. [Online]. Available: <https://arxiv.org/abs/2311.07199>
- [21] T. Fang, Y. Mao, S. Shen, Z. Zhu, and B. Clerckx, "Fully connected reconfigurable intelligent surface aided rate-splitting multiple access for multi-user multi-antenna transmission," in *IEEE Int. Conf. Commun. Workshop.*, Seoul, Korea, May 2022, pp. 675–680.
- [22] H. Li, S. Shen, and B. Clerckx, "Synergizing beyond diagonal reconfigurable intelligent surface and rate-splitting multiple access," *IEEE Trans. Wireless Commun.*, vol. 23, no. 8, pp. 8717–8729, Aug. 2024.
- [23] —, "A dynamic grouping strategy for beyond diagonal reconfigurable intelligent surfaces with hybrid transmitting and reflecting mode," *IEEE Trans. Vehicular Tech.*, vol. 72, no. 12, pp. 16748–16753, Dec. 2023.
- [24] M. Nerini, S. Shen, and B. Clerckx, "Static grouping strategy design for beyond diagonal reconfigurable intelligent surfaces," *IEEE Commun. Lett.*, vol. 28, no. 7, pp. 1708–1712, Jul. 2024.
- [25] M. Nerini, G. Ghiaasi, and B. Clerckx, "Localized and distributed beyond diagonal reconfigurable intelligent surfaces with lossy

- interconnections: Modeling and optimization,” 2024. [Online]. Available: <https://arxiv.org/abs/2402.05881>
- [26] M. Nerini and B. Clerckx, “Physically consistent modeling of stacked intelligent metasurfaces implemented with beyond diagonal RIS,” *IEEE Comm. Lett.*, vol. 28, no. 7, pp. 1693–1697, Jul. 2024.
- [27] H. Li, S. Shen, Y. Zhang, and B. Clerckx, “Channel estimation and beamforming for beyond diagonal reconfigurable intelligent surfaces,” *IEEE Trans. Signal Process.*, vol. 72, pp. 3318–3332, 2024.
- [28] M. Nerini, S. Shen, and B. Clerckx, “Closed-form global optimization of beyond diagonal reconfigurable intelligent surfaces,” *IEEE Trans. Wireless Commun.*, vol. 23, no. 2, pp. 1037–1051, Feb. 2024.
- [29] T. Fang and Y. Mao, “A low-complexity beamforming design for beyond-diagonal RIS aided multi-user networks,” *IEEE Commun. Lett.*, vol. 28, no. 1, pp. 203–207, 2024.
- [30] Y. Zhao, H. Li, M. Franceschetti, and B. Clerckx, “Channel shaping using beyond diagonal reconfigurable intelligent surface: Analysis, optimization, and enhanced flexibility,” 2024. [Online]. Available: <https://arxiv.org/abs/2407.15196>
- [31] Y. Zhou, Y. Liu, H. Li, Q. Wu, S. Shen, and B. Clerckx, “Optimizing power consumption, energy efficiency, and sum-rate using beyond diagonal RIS—a unified approach,” *IEEE Trans. Wireless Commun.*, vol. 23, no. 7, pp. 7423–7438, Jul. 2024.
- [32] M. Nerini, S. Shen, H. Li, M. Di Renzo, and B. Clerckx, “A universal framework for multiport network analysis of reconfigurable intelligent surfaces,” *IEEE Trans. Wireless Commun.*, vol. 23, no. 10, pp. 14 575–14 590, Oct. 2024.
- [33] D. Pozar, *Microwave Engineering*. John Wiley & Sons, 2011.
- [34] J. Papandriopoulos and J. S. Evans, “SCALE: A low-complexity distributed protocol for spectrum balancing in multiuser DSL networks,” *IEEE Trans. Inf. Theory*, vol. 55, no. 8, pp. 3711–3724, Aug. 2009.
- [35] Q. Shi, M. Razaviyayn, Z.-Q. Luo, and C. He, “An iteratively weighted mmse approach to distributed sum-utility maximization for a MIMO interfering broadcast channel,” *IEEE Trans. Signal Process.*, vol. 59, no. 9, pp. 4331–4340, Sept. 2011.
- [36] A. Wiesel, Y. Eldar, and S. Shamai, “Linear precoding via conic optimization for fixed MIMO receivers,” *IEEE Trans. Signal Process.*, vol. 54, no. 1, pp. 161–176, Jan. 2006.
- [37] W. Yu and T. Lan, “Transmitter optimization for the multi-antenna downlink with per-antenna power constraints,” *IEEE Trans. Signal Process.*, vol. 55, no. 6, pp. 2646–2660, Jun. 2007.
- [38] K. Shen and W. Yu, “Fractional programming for communication systems—part I: Power control and beamforming,” *IEEE Trans. Signal Process.*, vol. 66, no. 10, pp. 2616–2630, May 2018.
- [39] —, “Fractional programming for communication systems—part II: Uplink scheduling via matching,” *IEEE Transactions on Signal Processing*, vol. 66, no. 10, pp. 2631–2644, May 2018.
- [40] S. Boyd, N. Parikh, E. Chu, B. Peleato, J. Eckstein *et al.*, “Distributed optimization and statistical learning via the alternating direction method of multipliers,” *Found. Trends Mach. Learn.*, vol. 3, no. 1, pp. 1–122, 2011.
- [41] Y.-F. Liu, T.-H. Chang, M. Hong, Z. Wu, A. Man-Cho So, E. A. Jorswieck, and W. Yu, “A survey of recent advances in optimization methods for wireless communications,” *IEEE J. Sel. Areas Commun.*, vol. 42, no. 11, pp. 2992–3031, Nov. 2024.
- [42] W. Gao, D. Goldfarb, and F. E. Curtis, “ADMM for multiaffine constrained optimization,” *Optim. Methods Softw.*, vol. 35, no. 2, pp. 257–303, 2020.
- [43] J. Zhang, Y. Duan, Y. Lu, M. K. Ng, and H. Chang, “Bilinear constraint based ADMM for mixed poisson-gaussian noise removal,” *Inverse Problems and Imaging*, vol. 15, no. 2, pp. 339–366, 2021.
- [44] K. Shen, W. Yu, L. Zhao, and D. P. Palomar, “Optimization of MIMO device-to-device networks via matrix fractional programming: A minorization–maximization approach,” *IEEE/ACM Trans. Netw.*, vol. 27, no. 5, pp. 2164–2177, Oct. 2019.
- [45] M. Hong, Z.-Q. Luo, and M. Razaviyayn, “Convergence analysis of alternating direction method of multipliers for a family of nonconvex problems,” *SIAM J. Optim.*, vol. 26, no. 1, pp. 337–364, 2016.
- [46] Y. Wang, W. Yin, and J. Zeng, “Global convergence of ADMM in nonconvex nonsmooth optimization,” *J. Sci. Comput.*, vol. 78, no. 1, pp. 29–63, 2019.